EVALUATION OF THE INFLUENCE OF LOW-FREQUENCY ATMOSPHERE-OCEAN OSCILLATIONS ON ANNUAL FLOODS IN GODAVARI AND NARMADA RIVER BASINS

(Project Reference Code: NIH/SWHD/NIH/18-21)

FINAL REPORT

(2018 – 21)

Prepared by

Dr. Sunil Gurrapu

Scientist 'C'

SURFACE WATER HYDROLOGY DIVISION (SWHD)

NATIONAL INSTITUTE OF HYDROLOGY, ROORKEE

UTTARAKHAND – 247 667

EVALUATION OF THE INFLUENCE OF LOW-FREQUENCY ATMOSPHERE-OCEAN OSCILLATIONS ON ANNUAL FLOODS IN GODAVARI AND NARMADA RIVER BASINS

(Project Reference Code: NIH/SWHD/NIH/18-21)

FINAL REPORT

(2018 – 21)

PROJECT PARTICULARS

Project Team:	Dr. Sunil Gurrapu, *Scientist 'C' (PI)* Dr. Ashwini Ranade, *Scientist 'D'* Mr. Jagadish Prasad Patra, *Scientist 'D'*
Type of Study:	Internal
Duration:	3 years
Date of Start:	1st November 2018
Date of Completion	31st October 2021

Evaluation of the Influence of Low-Frequency Atmosphere-Ocean Oscillations on Annual Floods in Godavari and Narmada River Basins

Project Report Prepared by

Dr. Sunil Gurrapu, Scientist 'C'

Surface Water Hydrology Division

National Institute of Hydrology, Roorkee

Uttarakhand – 247667

For any Queries: gurrapus@gmail.com

©NIH Roorkee, March 2022

PREFACE

Indian summer monsoon rainfall is strongly influenced by various large-scale atmosphere-ocean oscillations, i.e. teleconnections. For example, several researchers have shown that the negative phase of the pacific decadal oscillation (PDO) and the La Niña episodes of El Niño-Southern Oscillation (ENSO) produce higher magnitude rainfall, i.e. wet years compared to that of the corresponding positive phase of PDO or the El Niño episodes of ENSO. In addition, La Niña episodes co-occurring during the negative PDO phase produced a much higher magnitude rainfall, i.e. abnormally wet years. So, it is imperative to have better knowledge of the magnitude and frequency of annual peak flows or floods in the watersheds of Indian subcontinent for optimal planning and design of various water resources & transportation infrastructure, and for optimal planning and management of reservoir operations. Traditionally, such information is estimated using flood frequency analysis (FFA) for small and medium sized projects. A general assumption made in FFA is that the annual peak flow series is independent and identically distributed. Violation of this assumption may lead to gross under-estimation or over-estimation of the true long-term flood risk. So, this study aims to fill this gap with a primary objective of evaluating the influence of teleconnections on annual floods in Godavari and Narmada River basins.

This study identifies how the flood risk in Godavari and Narmada River basins is modified by these teleconnections, specifically low-frequency PDO, ENSO and Indian Ocean Dipole (IOD). The daily streamflow data used in the analyses was collected from India-WRIS (https://indiawris.gov.in/wris/), and the monthly or annual indices of low-frequency atmosphere-ocean oscillations PDO, ENSO, & IDO were collected from the various global sources including (*i*) National Oceanic and Atmospheric Administration (NOAA), USA (https://www.ncdc.noaa.gov/teleconnections/pdo/), (*ii*) Climate Research Unit (CRU), University of Eastern Anglia (https://crudata.uea.ac.uk/cru/data/soi/), etc. The annual maximum daily averaged streamflow datasets were stratified according to the phases of PDO, ENSO & IOD and fit by a suitable probability distribution. A suitable probability distribution was chosen based on a Kolmogorov-Smirnov test. The stratified datasets are then analysed by constructing quantile-quantile plots, flood frequency curves, etc. Flood ratio approach was also adopted to evaluate the regional influence of these teleconnections. The results indicate that the flood magnitude at majority of the selected gauging sites in the Godavari River Basin is

significantly influenced by the phases of PDO and ENSO. In this basin, higher (lower) magnitude floods are associated with negative (positive) phase of PDO and La Niña (El Niño) episodes. In contrast, such an influence could not be seen at the gauging sites of Narmada River Basin, except for a very few sites. In general, the influence of these teleconnections is spatially variable and so the contrasting results. Although the annual floods at majority of the selected sites are significantly influenced by ENSO & PDO, none of them show the influence of IOD.

This report has been prepared by **Dr. Sunil Gurrapu** (PI), Scientist 'C', Surface Water Hydrology Division (SWHD), with technical support from **Dr. Ashwini Ranade** (Co-PI), Scientist 'D', SWHD, and **Er. J P Patra** (Co-PI), Scientist 'D', SWHD. This is an internal research project with financial support (if any), although no expenses were incurred during the course of this project work, from National Institute of Hydrology, Roorkee. The overall guidance was provided by **Dr. Rakesh Kumar**, former Head, SWHD, and **Dr. A K Lohani**, Head, SWHD, NIH Roorkee.

LIST OF FIGURES

	left hand corners, together with record length. Shown in the lower right corner are the statistical significance levels of the permutations test. NS indicated not significant
Figure 13	Quantile-Quantile plots based on annual peak flows (m^3/sec) stratified according to El Niño and La Niña episodes for the 46 streamflow gauges in Godavari River basin. Shown in blue are the 1:1 lines. The stations codes are shown in the upper left hand corners, together with record length. Shown in the lower right corner are the statistical significance levels of the permutations test. NS indicated not significant.
Figure 14	Quantile-Quantile plots based on annual peak flows (m^3/sec) stratified according to El Niño and La Niña episodes for the 46 streamflow gauges in Narmada River basin. Shown in blue are the 1:1 lines. The stations codes are shown in the upper left hand corners, together with record length. Shown in the lower right corner are the statistical significance levels of the permutations test. NS indicated not significant
Figure 15	Quantile-Quantile plots based on annual peak flows (m^3/sec) stratified according to positive and negative phases of Indian Ocean Dipole (IOD) for the 46 streamflow gauges in Godavari River basin. Shown in blue are the 1:1 lines. The stations codes are shown in the upper left hand corners, together with record length. Shown in the lower right corner are the statistical significance levels of the permutations test. NS indicated not significant
Figure 16	Quantile-Quantile plots based on annual peak flows (m^3/sec) stratified according to positive and negative phases of Indian Ocean Dipole (IOD) for the 46 streamflow gauges in Narmada River basin. Shown in blue are the 1:1 lines. The stations codes are shown in the upper left hand corners, together with record length. Shown in the lower right corner are the statistical significance levels of the permutations test. NS indicated not significant.
Figure 17	3-Parameter Lognormal (LN3) flood frequency curves (solid lines) and their 90% confidence intervals (dashed lines) for the annual peak flows in selected gauges of Godavari River Basin, stratified according to negative (Aug–Oct averaged PDO index < -0.05) and positive (Aug–Oct averaged PDO index > 0.05) PDO phases of the Pacific Decadal Oscillation (PDO). (a) Pachegaon, (b) Purna, (c) Kanergaon, and (d) Wairagarh
Figure 18	3-Parameter Lognormal (LN3) flood frequency curves (solid lines) and their 90% confidence intervals (dashed lines) for the annual peak flows in selected gauges of Narmada River Basin, stratified according to negative (Aug–Oct averaged PDO index

LIST OF TABLES

TABLE OF CONTENTS

SUMMARY

Indian summer monsoon rainfall is strongly influenced by the large-scale atmosphere-ocean oscillations including Pacific Decadal Oscillation (PDO), El Niño-Southern Oscillation (ENSO), and Indian Ocean Dipole (IOD), among many other patterns. Researchers have shown that the negative phase of the PDO or the La Niña episodes of ENSO produce higher magnitude rainfall and hence wet years compared to that of the corresponding positive phase of PDO or the El Niño episodes of ENSO. La Niña episodes co-occurring during the negative PDO phase also produce higher magnitude rainfall or abnormally wet years. So, it is imperative to have better knowledge of the magnitude and frequency of annual peak flows or floods in the watersheds of Indian subcontinent for optimal planning and design of various water resources & transportation infrastructure, and for optimal planning and management of reservoir operations. Traditionally, such information is estimated using flood frequency analysis (FFA) for small and medium sized projects. A general assumption made in FFA is that the annual peak flows are independent and identically distributed. Violation of this assumption may led to gross under-estimation or over-estimation of the true long-term flood risk. This study identifies how the flood risk in Godavari and Narmada River basins is modified by these teleconnections, specifically low-frequency PDO, ENSO and IOD. Annual maximum daily averaged streamflow datasets were stratified according to the phases of PDO, ENSO & IOD and fit by a suitable probability distribution. A suitable probability distribution was chosen based on Kolmogorov-Smirnov test.

The results indicate that the flood risk at most of the selected gauges in Godavari Basin is significantly influenced by PDO and ENSO, magnitudes are substantially different in different phases of these oscillations. In Godavari Basin, higher magnitude floods are associated with negative phase of PDO and La Niña episodes of ENSO. The results also indicate that the PDO phase modulates the effects of ENSO, i.e. floods during La Niña episodes occurring during negative PDO phase have higher magnitudes than floods during La Niña episodes occurring during the positive PDO phase. In contrast, this influence is not observed at the gauging sites of Narmada River basin, except for a few sites. In general, the influence of these teleconnections is spatially variable and so the contrasting results. Although the annual floods at majority of the selected sites are significantly influenced by ENSO & PDO, none of them show the influence of IOD. As an example, the influence of PDO on annual floods in a few selected gauging sites of Godavari Basin is shown in the figure below.

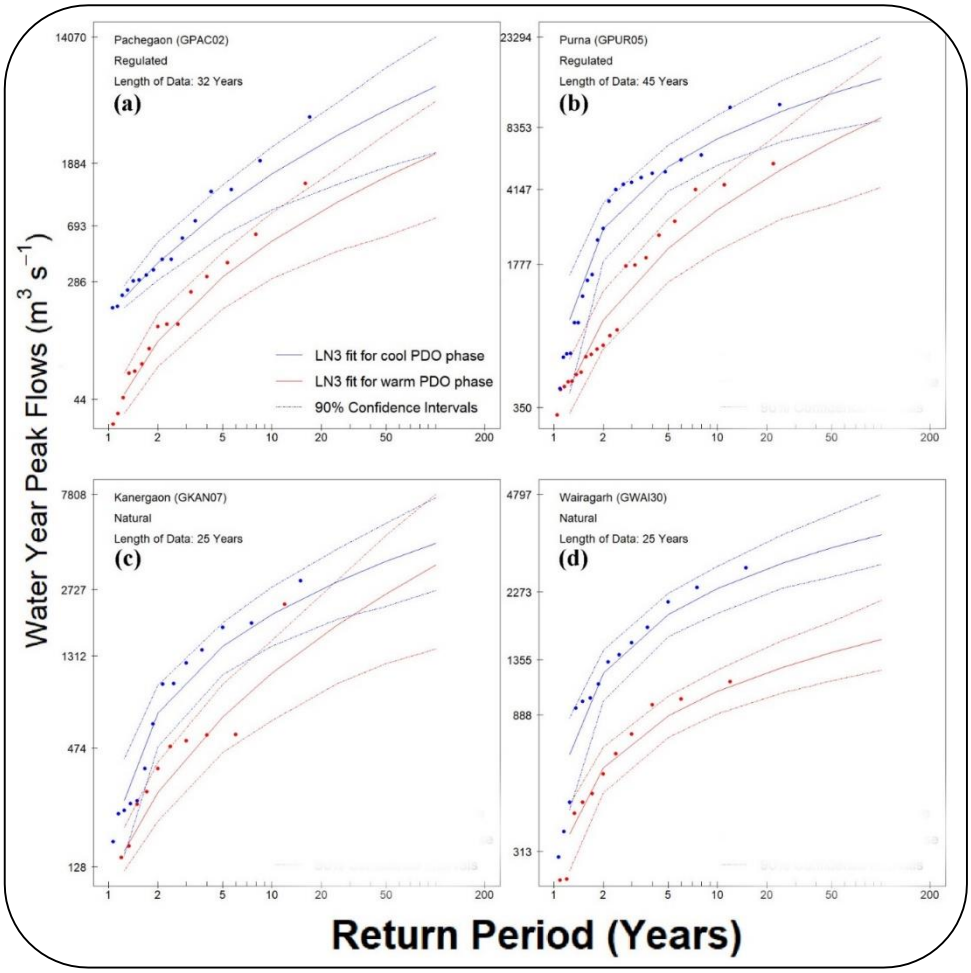

Figure A: The influence of PDO on the flood frequency and flood magnitude, after stratifying the peak flow records based on the PDO index, at selected gauging sites of Godavari River Basin, (a) Pachegaon, (b) Purna, (c) Kanergaon, and (d) Wairagarh. Detailed explanation and description of this figure may be found in the report and in Figure 23.

Keywords: Pacific Decadal Oscillation, El Niño-Southern Oscillation, Indian Ocean Dipole, Flood Frequency, Quantile-Quantile Plots, Non-Stationarity, Large-scale low-frequency atmosphere-ocean oscillations.

INTRODUCTION

Globally, floods are ranked among the largest and costliest natural disasters having major impact on various economic sectors (Bryant, 2005). In India, flooding is one of the three prominent climate extremes, other two being droughts and cyclones (Bhattacharya & Das, 2007). Majority of flooding in Indian watersheds occurs during summer monsoon months due to uneven distribution of rainfall. For example, recent devastating floods in Kerala were in response to the abnormally high rainfall received within a short period of 3 days, i.e. during 15th to 17th August 2018. Approximately 80% of rainfall over the Indian subcontinent is received during summer monsoon. Summer monsoon rainfall being the major source of water input to the Indian subcontinent, optimal design and operation of water resources infrastructure (e.g. major dams) is very much essential.

Indian summer monsoon is substantially influenced by several low-frequency atmosphere-ocean oscillations including Pacific Decadal Oscillation (PDO), El Niño-Southern Oscillation (ENSO), Indian Ocean Dipole (IOD), Atlantic Multidecadal Oscillation (AMO), etc. (e.g. Roy et al., 2003; Sajani et al., 2007; Krishnamurthy & Krishnamurthy, 2013a; 2013b; Li et al., 2017; Saini et al., 2022). For example, Krishnamurthy & Krishnamurthy (2013a) identified that the warm phase of PDO is associated with the rainfall deficit over Indian subcontinent, whereas the cool phase of PDO is associated with the rainfall excess (Figure A1). A similar relationship is identified with El Niño and La Niña episodes of ENSO pattern (e.g. Krishnamurthy & Krishnamurthy, 2013a; Saini et al., 2022). Despite these studies on teleconnections and Indian summer monsoon rainfall (ISMR), there has been little work done on the teleconnections between these low-frequency atmosphere-ocean oscillations and annual mean and/or peak streamflow in the watersheds of Indian subcontinent. Henceforth, this study explores the teleconnections between large-scale atmosphere-ocean oscillations, the PDO, ENSO & IOD and the annual peak streamflow in Godavari and Narmada River basins. Knowledge of the magnitude and frequency of annual peak flows (floods) in these watersheds plays an important role in optimal planning and design of various infrastructure, and informs adaptive management policy for better reservoir operations.

Traditionally, flood frequency analysis is a widely used technique for effective planning and design of water resources and transportation infrastructure. One primary assumption made in FFA is that the annual peak flow series at any site is independent and identically distributed (*i.i.d*) and the system fluctuates within a fixed envelope of variability, i.e. stationarity

assumption (e.g. Milly et al. 2008). However, several studies across the globe highlight the potential inadequacy of traditional flood frequency analysis and argue that the *i.i.d.* assumption can no longer be considered valid (e.g. Stedinger & Griffis 2008; Milly et al. 2008; Gurrapu et al. 2016; 2022). Gurrapu et al., (2016) demonstrated that the frequency of floods in the watersheds of western Canada is substantially impacted by a large-scale low-frequency PDO, where the negative phase of PDO produced higher magnitude floods and the positive phase of PDO produced relatively lesser magnitude floods. In a similar study, Franks (2002) and Kiem et al (2003) demonstrated that the frequency of floods in New South Wales, Australia is impacted by Inter-Decadal Pacific Oscillation (IPO) and ENSO. They suggest that annual peak flow data should be assessed as a function of the causal climatological factors that affect regional climates. Ward et al. (2014) determined that La Niña episodes produce higher annual floods compared to El Niño episodes in majority of the river basins across the globe, whereas few basins show the opposite relation. In another study, Andrews et al. (2004) determine that El Niño episodes produced higher annual floods along the California coast, USA. Therefore, knowledge of climate state with regard to regional teleconnection patterns is required before performing FFA.

In this study, the annual peak flows or floods (i.e. annual maximum daily streamflow) in Godavari and Narmada River basins were analyzed with the hypothesis that they are influenced by the low-frequency atmosphere oscillations originating in the equatorial Pacific and Indian Oceans, including PDO, ENSO and IOD. This study was motivated by the observation that such teleconnections are not yet a key ingredient in planning and design of regional water resources and/or transportation infrastructure. In specific, this study evaluates the influence of PDO, ENSO and IOD on the magnitude and frequency of annual peak flows in selected streamflow gauging stations spread across Godavari and Narmada River basins. This study is first of its kind to evaluate the impact of these low frequency oscillations, which are known to substantially control the magnitude and frequency of ISMR, on the annual peak flows in Indian watersheds. The necessity of such a study is illustrated by the annual hydrographs of selected streamflow gauging sites which show higher peak flow during the negative PDO phase (lowest magnitude PDO index during the period of flow record) and lower peak flow during positive PDO phase (highest magnitude PDO index during the period of flow record). For example, the annual discharge and the annual peak flow at a gauging site near Bhatpalli (GBHA21) on Pranhitha River, a sub-basin of Godavari River Basin in 2008, the year with the lowest negative PDO index during 1986 - 2017, were substantially higher than those

in 1987, the year with the highest positive PDO index, Figure 1a. Similarly, the annual discharge and the annual peak flow at a gauging site near Pati (NPAT16) on Goi River, a sub-basin of Narmada River Basin in 2008, the year with the lowest negative PDO index during 1999 - 2016, were substantially higher than those in 2015, the year with the highest positive PDO index, Figure 1b.

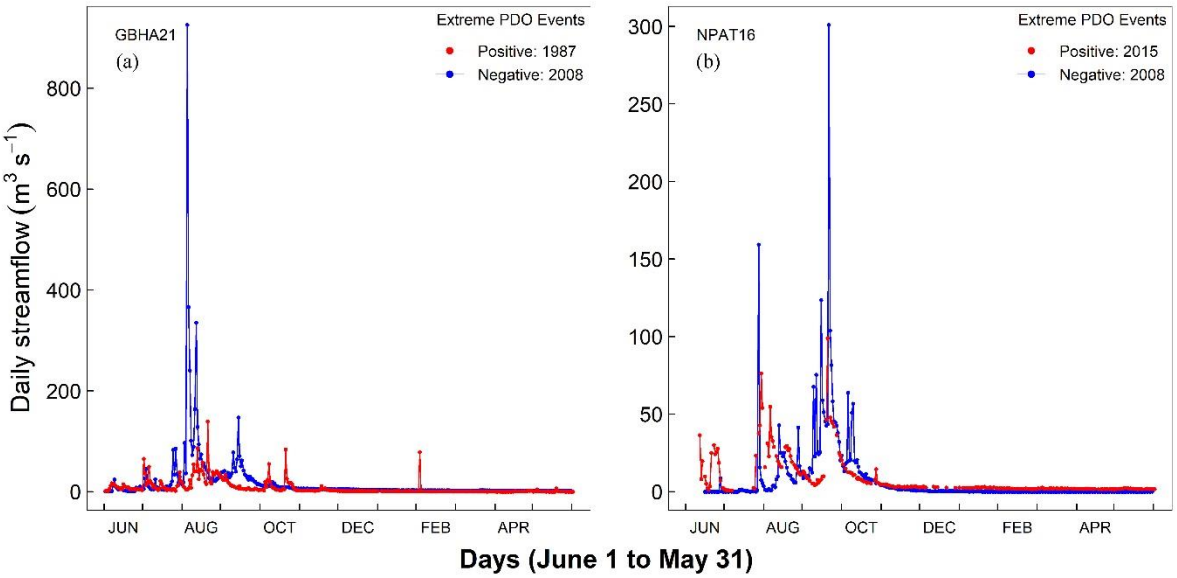

Figure 1 Response hydrograph of the (a) Pranhitha River at Bhatpalli (GBHA21, Godavari River Basin) for 2008, the year with most negative PDO index (blue line), and for 1987, the year with the most positive PDO index (red line) during the period of flow record 1986 – 2017; and (b) Goi River at Pati (NPAT16, Narmada River Basin) for 2008, the year with most negative PDO index (blue line), and for 2008, the year with the most positive PDO index (red line) during the period of flow record 1999 – 2016.

OBJECTIVES

1. Analyze annual peak flows in the rivers of Indian subcontinent, the main objective of this study is evaluate the stationarity assumption made in flood frequency studies.
2. Evaluate the influence of various low-frequency atmosphere-ocean oscillations on flood magnitude and frequency.
    a. Pacific Decadal Oscillation (PDO) and El Nino Southern Oscillation (ENSO) are large-scale climate patterns occurring over the Pacific Ocean.
    b. They are quantified into indices at a monthly scale, based on the varying sea surface temperature and pressure over the equatorial Pacific Ocean. Such

indices are available from various institutes across the world including (i) Joint Institute for the study of Atmosphere and the Ocean (JISAO), USA, (ii) Climate Research Unit (CRU), University of Eastern Anglia, UK, (iii) National Oceanic and Atmospheric Administration (NOAA), USA.

c. In this objective, we evaluate correlations between these indices and annual peak flow. We also aim to quantify their influence on annual floods and provide a correction factor to account for the non-stationarity.

STUDY AREA AND DATA

To evaluate the influence of the PDO on annual floods (i.e. annual maximum daily streamflow), recorded daily streamflow data from 64 streamflow gauging stations (Figure 2 & Table 1) spread across Godavari (46 gauges) and Narmada (18 gauges) river basins were chosen. Godavari River Basin is an east flowing river draining into the Bay of Bengal and is spread across the states of Maharashtra, Madhya Pradesh, Chhattisgarh, Odisha, Andhra Pradesh, Telangana, and Karnataka, whereas the Narmada River Basin is a west flowing river draining into the Arabian Sea and is spread across the states of Madhya Pradesh and Gujarat. All the selected gauging sites are operated and maintained by Central Water Commission (CWC) and the observed daily streamflow is available from Indi-WRIS (India Water Resources Information Systems) for free. These gauges were selected based on the available length of daily streamflow data, each station has at least 10-years of streamflow data, whether continuous or discontinuous. The gross drainage area of the selected sub-basins ranges between 787 km^2 and 3,07,800 km^2.

Annual peak flow in Godavari and Narmada Rivers typically occur during the southwest (i.e. during June – September) and/or northeast (i.e. during October – December) monsoon seasons, from high magnitude and/or high intensity rainfall. The time series of annual peak flows, maximum of the daily streamflow recorded during a water year starting from 1st June and ending on 31st May of the following year, at each station are extracted from the daily averaged streamflow records. At each gauging site, annual peak flow for any given year is extracted from all the available data, regardless of the missing data. Any year with missing daily streamflow data or with '0' annual mean streamflow is discarded and is not used in the analysis. Details of the selected streamflow gauging stations and the recorded daily streamflow data for all the selected gauging stations is downloaded freely from the India-WRIS website (https://indiawris.gov.in/wris/#/).

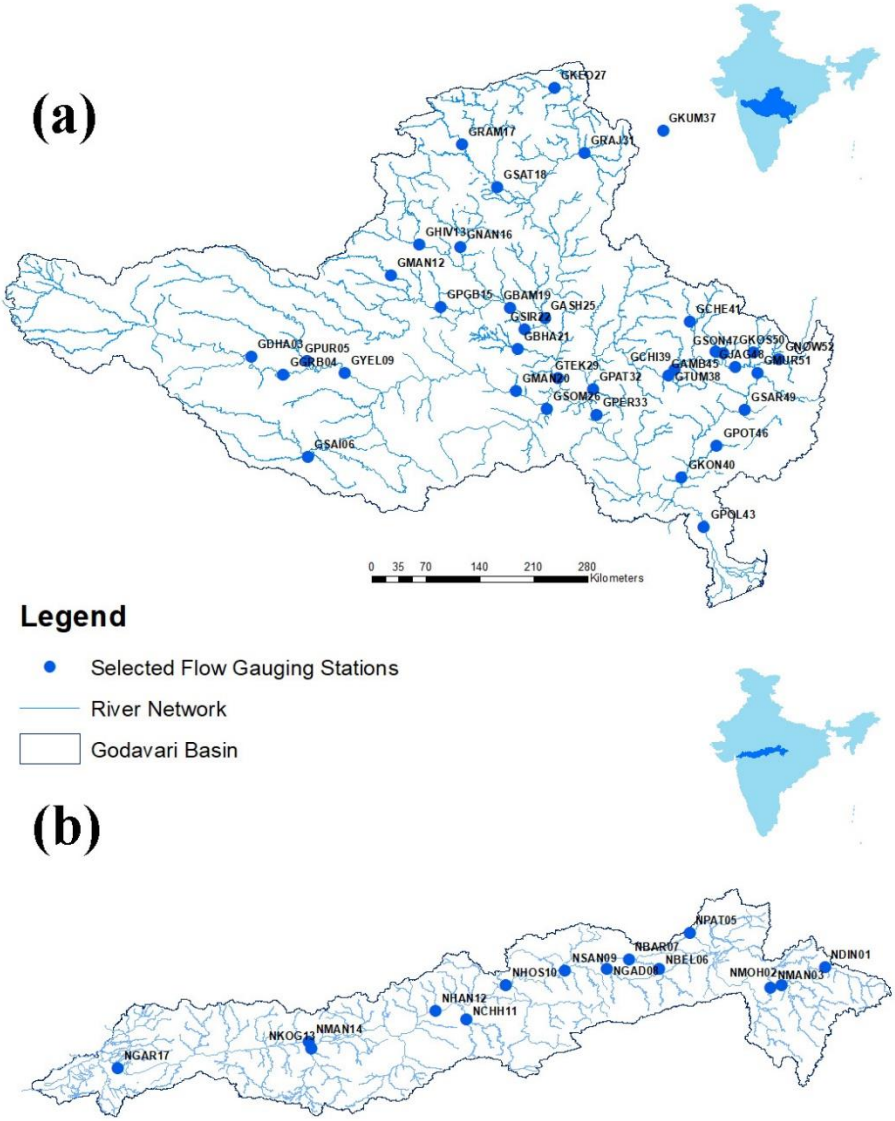

Figure 2. Locations of all the selected streamflow gauging stations from (a) Godavari and (b) Narmada River Basins.

To analyze the influence of the PDO on annual peak streamflow, August to October monthly averaged PDO index ($PDO_{Aug\text{-}Oct}$) from the Joint Institute for the Study of Atmosphere and Ocean (JISAO), University of Washington (http://jisao.washington.edu/pdo/) (Mantua et al., 1997), was used. The temporal variability of $PDO_{Aug\text{-}Oct}$ and the JISAO defined phases of PDO can be seen in Figure 3. In this study, the influence of PDO on annual flood was analysed based on the magnitude of PDO index, by categorizing them into positive (threshold value = 0.05) and negative (threshold value = −0.05) phases of PDO. To do so, the annual peak flow series at each station are stratified as the basin's hydrological response to positive ($PDO_{Aug\text{-}Oct} \geq 0.05$) and negative ($PDO_{Aug\text{-}Oct} \leq -0.05$) phases of the PDO (e.g. Gurrapu et al., 2016).

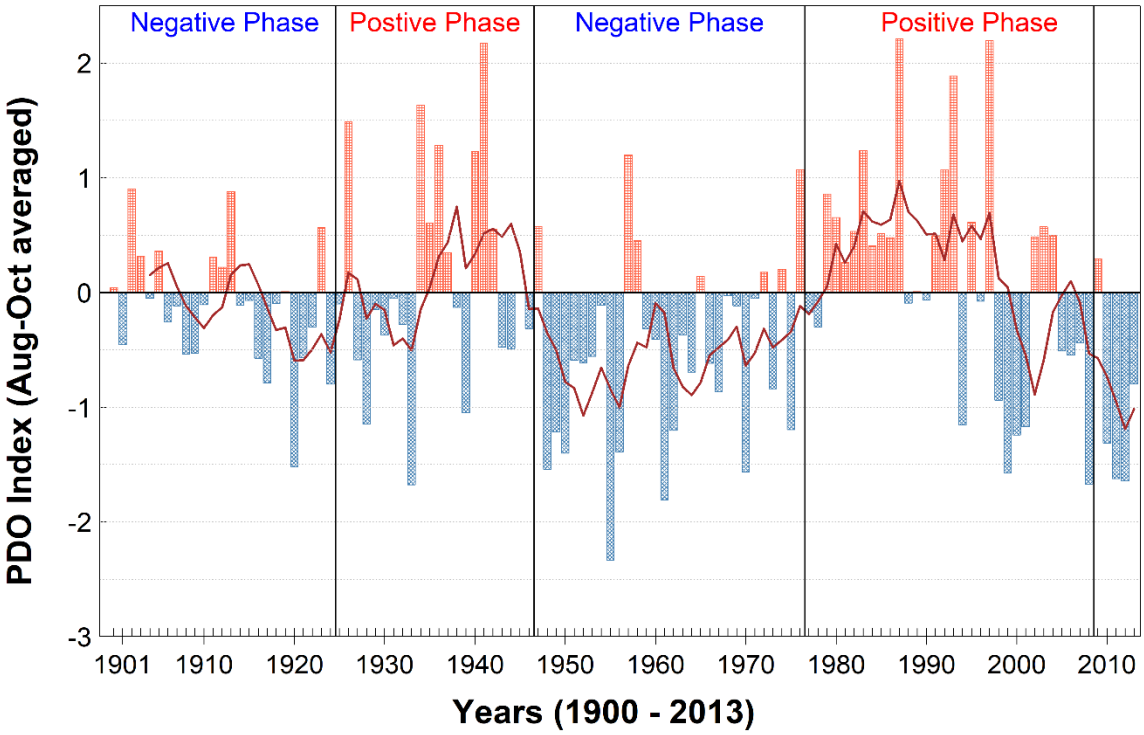

Figure 3. Variability in the Pacific Decadal Oscillation (PDO) as represented by the August to October averaged PDO index for the period 1900 to 2013, together with the 5-year running mean (dark red line).

In order to directly compare the results from the low-frequency PDO to those from the higher-frequency ENSO, its influence on annual peak streamflow is also analyzed. ESNO is quantified in several ways by various instituted across the globe. In this study, the Southern Oscillation Index (SOI) is used to categorize the ENSO events (Climate Research Unit, University of East Anglia, http://www.cru.uea.ac.uk/cru/data/soi/). In this study, June monthly SOI (SOI_{Jun}) is used to distinguish the ENSO episodes. The temporal variability of SOI_{Jun} over the past century can be seen in Figure 4. Using SOI_{Jun}, the annual peak flow series at each of the selected gauging stations are stratified as El Niño ($SOI_{Jun} \leq -0.05$), La Niña ($SOI_{Jun} \geq 0.05$) or neutral-year ($-0.05 < SOI_{Jun} < 0.05$) flows, Figure 4.

In addition to these two indices, the influence of Indian Ocean Dipole (IOD) on annual peak flows is also evaluated. Sustained changes in the difference between sea surface temperatures of the tropical western and eastern Indian Ocean are known as IOD, more details of this oscillation are available at www.bom.gov.au/climate/iod/. IOD is quantified by Dipole Mode Index (DMI; Saji et al., 1999), and is freely available from Earth Systems Research Laboratory (ESRL), National Oceanic and Atmospheric Administration (NOAA), USA. DMI

is computed at a monthly timescale and in this study, September to November averaged DMI ($DMI_{Sep-Nov}$) is used to evaluate the influence of DMI on annual floods.

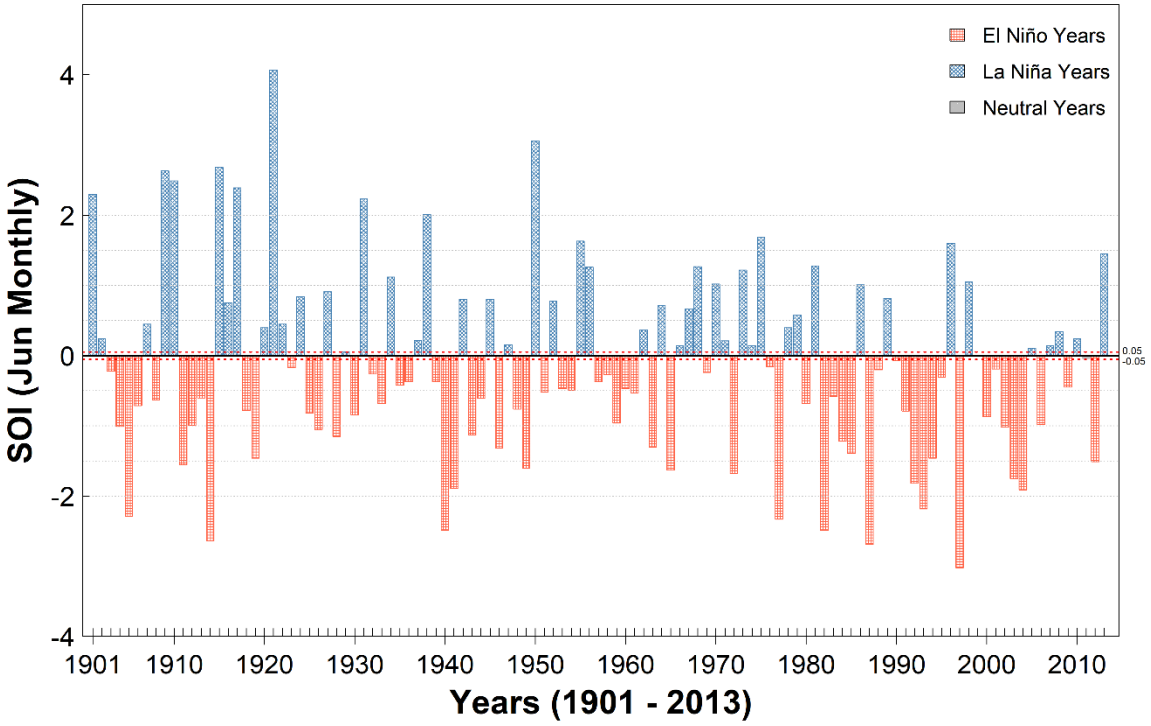

Figure 4. Variability in the El Niño-Southern Oscillation (ENSO) as represented by the annual averaged Southern Oscillation Index (SOI) index for the period 1901 to 2013, together with the lower and upper limits for categorizing into El Niño and La Niña episodes.

Table 1. List of the 64 selected streamflow gauges in Godavari and Narmada basins from the IWRIS Database, with their Station codes, names, location and other important particulars.

#	IWRIS ID	Stn ID	Station Name	Latitude	Longitude	Catchment Area	Tributary Name	Basin Name	Start Year	End Year	Gauge Type
1	AGU00D3	GPAC02	Pachegaon	19.53	74.83	5800	Pravara	Godavari	1979	2015	Regulated
2	AG00059	GDHA03	Dhalegaon	19.23	76.36	30840	Godavari	Godavari	1965	2015	Regulated
3	AG000R6	GGRB04	G.R. Bridge	19.02	76.73	33934	Godavari	Godavari	1976	2015	Regulated
4	AGR00A5	GPUR05	Purna	19.18	77.01	15000	Purna	Godavari	1968	2015	Regulated
5	AGP00N8	GSAI06	Saigaon	18.06	77.02	9960	Manjira	Godavari	1965	2015	Regulated
6	AGH32R8	GKAN07	Kanergaon	19.96	77.15	3515	Pranhitha	Godavari	1991	2017	Natural
7	AG000P3	GYEL09	Yelli	19.04	77.45	53630	Godavari	Godavari	1976	2015	Regulated
8	AGP10F7	GBET10	Betmogra	18.71	77.54	2105	Manjira	Godavari	1997	2015	Natural
9	AGP20F4	GDEG11	Degloor	18.56	77.58	1900	Manjira	Godavari	1984	2015	Regulated
10	AGH35G0	GMAN12	Mangrul	20.19	77.99	2500	Pranhitha	Godavari	1992	2017	Natural
11	AGH30Q1	GHIV13	Hivra	20.55	78.32	10240	Pranhitha	Godavari	1987	2017	Regulated
12	AGM00G6	GGAN14	Gandlapet	18.8	78.44	1360	Peddavagu	Godavari	1986	2015	Natural
13	AGH32D5	GPGB15	P.G. (Penganga) Bridge	19.82	78.57	18441	Pranhitha	Godavari	1965	2017	Regulated
14	AGH3AF4	GNAN16	Nandgaon	20.52	78.8	4580	Pranhitha	Godavari	1986	2017	Regulated
15	AGH4BQ3	GRAM17	Ramakona	21.72	78.82	2500	Pranhitha	Godavari	1986	2017	Natural
16	AGH4BF6	GSAT18	Satrapur	21.22	79.23	11100	Pranhitha	Godavari	1984	2017	Regulated
17	AGH30E2	GBAM19	Bamini (Balharsha)	19.81	79.38	46020	Pranhitha	Godavari	1965	2017	Regulated

18	AG000J3	GMAN20	Mancherial	18.83	79.45	102900	Godavari	Godavari	1965	2015	Regulated
19	AGH10L0	GBHA21	Bhatpalli	19.32	79.47	3100	Pranhitha	Godavari	1986	2017	Regulated
20	AGH30B6	GSIR22	Sirpur	19.55	79.55	47500	Pranhitha	Godavari	1965	2015	Regulated
21	AGHA1Q4	GRAJ23	Rajoli	20.05	79.71	1900	Pranhitha	Godavari	1986	2017	Natural
22	AGR10C6	GZAR24	Zari	19.39	79.77	5550	Purna	Godavari	1986	2015	Natural
23	AGH40A4	GASH25	Ashti	19.68	79.79	50990	Pranhitha	Godavari	1965	2017	Regulated
24	AGI00C3	GSOM26	Somanpally	18.62	79.81	12691	Maner	Godavari	1964	2014	Regulated
25	AGH40V3	GKEO27	Keolari	22.38	79.9	2970	Pranhitha	Godavari	1986	2017	Regulated
26	AGH49I1	GSAL28	Salebardi	20.91	79.93	1800	Pranhitha	Godavari	1985	2017	Natural
27	AGH00C4	GTEK29	Tekra	18.98	79.94	108780	Pranhitha	Godavari	1964	2017	Regulated
28	AGH46D4	GWAI30	Wairagarh	20.42	80.08	2600	Pranhitha	Godavari	1992	2017	Natural
29	AGH4MC3	GRAJ31	Rajegaon	21.62	80.25	5380	Pranhitha	Godavari	1985	2017	Regulated
30	AGG00B5	GPAT32	Pathagudem	18.85	80.35	40000	Indravathi	Godavari	1965	2015	Regulated
31	AG000G7	GPER33	Perur	18.55	80.39	268200	Godavari	Godavari	1965	2015	Regulated
32	SANGAM	GSAN35	Sangam	17.58	80.78	1565	Murredu	Godavari	1996	2014	Natural
33	AGH40R6	GKUM37	Kumhari	21.88	81.17	8070	Pranhitha	Godavari	1986	2017	Regulated
34	AGG60B1	GTUM38	Tumnar	19.01	81.23	1700	Indravathi	Godavari	1989	2015	Natural
35	AGG00N7	GCHI39	Chindnar	19.08	81.3	17270	Indravathi	Godavari	1971	2015	Regulated
36	AGC00C5	GKON40	Konta	17.82	81.39	19550	Sabari	Godavari	1964	2015	Regulated
37	CHERRIBEDA	GCHE41	Cherribeda	19.64	81.49	890	Indravathi	Godavari	1996	2014	Natural

38	AG000C3	GPOL43	Polavaram	17.24	81.65	307800	Godavari	Godavari	1965	2015	Regulated
39	AGC90C8	GAMB45	Ambabal	19.29	81.79	1968	Indravathi	Godavari	1989	2015	Natural
40	AGC20H2	GPOT46	Potteru	18.19	81.8	1120	Sabari	Godavari	1989	2015	Regulated
41	AGG91F2	GSON47	Sonarpal	19.27	81.88	1523	Markandi	Godavari	1989	2015	Natural
42	AGG00R9	GJAG48	Jagdalpur	19.11	82.02	7380	Indravathi	Godavari	1964	2015	Regulated
43	AGC00N4	GSAR49	Saradaput	18.61	82.13	3047	Sabari	Godavari	1968	2015	Regulated
44	KOSAGUMDA	GKOS50	Kosagumda	19.28	82.23	1635	Indravathi	Godavari	1996	2014	Natural
45	AGC40E9	GMUR51	Murthahandi	19.04	82.28		Indravathi	Godavari	1979	2015	Regulated
46	AGG00U7	GNOW52	Nowrangpur	19.2	82.53	3445	Indravathi	Godavari	1965	2015	Regulated
47	10215001	NDIN01	Dindori	22.95	81.08	2292	Narmada	Narmada	1988	2016	Regulated
48	10215004	NMOH02	Mohgaon	22.76	80.62	3919	Burhner	Narmada	1977	2016	Regulated
49	10215002	NMAN03	Manot	22.74	80.51	4667	Narmada	Narmada	1976	2016	Regulated
50	NCA SITE	NBAM04	Bamni Banjar	22.48	80.38	1864	Banjar	Narmada	1972	2016	Natural
51	10215009	NPAT05	Patan	23.31	79.66	3950	Heran	Narmada	1979	2016	Regulated
52	10215010	NBEL06	Belkheri	22.93	79.34	1508	Sher	Narmada	1977	2016	Natural
53	10215011	NBAR07	Barman at Narmada (Barmanghat)	23.03	79.02	26453	Narmada	Narmada	1971	2016	Regulated
54	10215012	NGAD08	Gadarwara	22.93	78.79	2270	Shakkar	Narmada	1977	2016	Natural
55	10215013	NSAN09	Sandia	22.92	78.35	33953	Narmada	Narmada	1978	2016	Regulated
56	10215019	NHOS10	Hoshangabad	22.76	77.73	44548	Narmada	Narmada	1972	2016	Regulated
57	10215020	NCHH11	Chhidgaon	22.4	77.31	1729	Ganjal	Narmada	1976	2016	Natural

58	10215022	NHAN12	Handia	22.49	76.99	54027	Narmada	Narmada	1977	2016	Regulated
59	10215025	NKOG13	Kogaon	22.1	75.68	3919	Kundi	Narmada	1972	2016	Regulated
60	10215026	NMAN14	Mandleshwar	22.17	75.66	72809	Narmada	Narmada	1971	2016	Regulated
61	NCA DHULSAR	NDHU15	Dhulsar	22021	74.85	787	Uri	Narmada	1999	2016	Natural
62	NCA PATI	NPAT16	Pati	21.94	74.75	2151	Goi	Narmada	1999	2016	Natural
63	10215030	NGAR17	Garudeshwar	21.89	73.65	87892	Narmada	Narmada	1972	2016	Regulated
64	10215032	NCHA18	Chandwada	22.05	73.47	3846	Orsang	Narmada	1979	2015	Regulated

METHODS

First, to explore whether the magnitude of annual peak flows is related to the large-scale climate oscillations, the non-parametric Spearman's rank correlation coefficient (ρ) was computed to measure the strength of the correlation between the annual peak flows and the indices of PDO, ENSO (SOI) and IOD (DMI) at each of the 64 gauging stations. Rank-based Spearman's correlation was used because it is robust and is not affected by the distribution of the climate and hydrologic data (Woo and Thorne, 2003; Wilks, 2006). In this analysis, any correlation (Spearman's ρ) with *p*-value less than or equal to 0.1 is considered significant at 90% confidence level (i.e. based on two-tailed significance test with $\alpha = 0.05$). Full period of record was used throughout this study because it is the longest record lengths that enable detection of the impact of the low-frequency PDO.

To further explore if the peak flows stratified according to PDO phase came from the same population, the peak flow series of each phase of the PDO were ranked and quantile-quantile (Q-Q) plots were constructed based on the quantiles from each phase (Chambers et al., 1983; Helsel and Hirsch, 2002). For each of the 64 gauges, the ranked floods (quantiles) of the negative PDO phase (y-axis) were plotted against the ranked floods (quantiles) of the positive PDO phase (x-axis), (i.e., for an individual point (x_i, y_i) of the plot, x_i is the peak flow of the i^{th} ranked flood in the positive PDO phase, and y_i is the peak flow of the i^{th} ranked flood in the negative PDO phase). If the data length of peak flows is same for both phases, the peak flows were directly plotted against each other. If the data sets are not of equal size, the quantiles were picked to correspond to the sorted values from the smaller data set and then quantiles for the larger data set were interpolated. The datasets can be assumed to be from the same population if the points fall along the 1:1 line. If the ratio $r_i = (y_i / x_i)$ of the i^{th} ranked floods is greater than 1, then the i^{th} ranked flood in the negative PDO phase is higher than that in the positive PDO phase. Values of r_i less than 1 indicate that the i^{th} ranked flood in the positive PDO phase is higher than that in the negative PDO phase. If the PDO phase has no effect on the magnitudes of the floods, the mean ratio *R* for a given gauge should be approximately 1. For each record, the significance of *R* was tested at the 0.1 significance level using a two-sided permutation test with 10,000 iterations (Manly, 2007).

The impact of the PDO on peak flows also was investigated using flood frequency curves fitted to the annual peak flow series stratified according to PDO phases, and 90%

confidence intervals were constructed (USGS, 1982) for all 50 records. If the 90% confidence intervals of the flood frequency curves separate, it cannot be assumed that the annual peak flow series is *i.i.d.* (Franks and Kuczera, 2002). The Kolmogorov-Smirnov goodness-of-fit test was used to determine the probability distribution that best represents the annual peak flow series. EasyfitXL 5.5® was used to test six distributions: Generalized Extreme Value (GEV), 2 & 3 Parameter Lognormal (LN & LN3), Log-Pearson III (LP3) and 2 & 3 Parameter Log-Logistic (LL & LL3). This analysis (results not shown) reveal that the annual peak flow series in both Godavari and Narmada River basins are generally best represented by the LN3 distribution.

Next, to further evaluate if the magnitude of peak flows differs between phases of the PDO, the ratio of the flood (fitted) quantiles in the negative phase to flood quantiles in the positive phase were computed for selected return periods, 2, 5, 10, 25, and 50. If this ratio, termed the flood ratio (Franks and Kuczera, 2002; Micevski et al., 2006), is greater than 1, it may be assumed that the higher magnitude peaks are more common in the negative PDO phase and vice-versa. In this analysis, we expect that peaks will be higher in the negative phase because it is known that Indian Summer Monsoon Rainfall is positively influenced by the negative PDO phase. A similar analysis was done to evaluate the influence of ENSO and IOD on the annual peak flows at the selected gauges. While the flood ratio is computed in the same way for evaluating the influence of the ENSO (SOI), it is computed as the ratio of flood quantile from La Niña episodes to the quantiles from El Niño episodes to evaluate the effect of ENSO.

RESULTS AND DISCUSSION

This study was motivated by the observation that the influence of low frequency oscillations upon flood risk is not yet a key ingredient in the planning and design of regional infrastructure, despite several studies showing strong correlations between ISMR and ENSO, PDO, & IOD. The effect of low-frequency oscillations on annual floods is evaluated in several ways and the results are discussed in this section.

Correlation Analysis: The influence of low-frequency analysis was first evaluated using a rank-based Spearman's correlations tests. First the annual peak flows at each gauging stations are standardized using Equation 1 and then their correlations with PDO was computed. As shown in Figure 5, annual streamflow in 13 gauging stations out of 46 selected gauges in Godavari river basin show statistically significant correlations with the August – October averaged PDO index. In all these stations, the annual peaks are negatively correlated, indicating

that the high magnitude floods are more common in the negative phase of PDO when compared to that of positive phase. These results concur with the observations made earlier researchers who indicate that the negative phase of PDO produces wet years, Figure A1. The statistically significant correlations of these 13 gauges ranged between -0.25 and -0.5, indicating that as much as 50% of the variability in annual peak streamflow at these stations can be explained by the low frequency PDO.

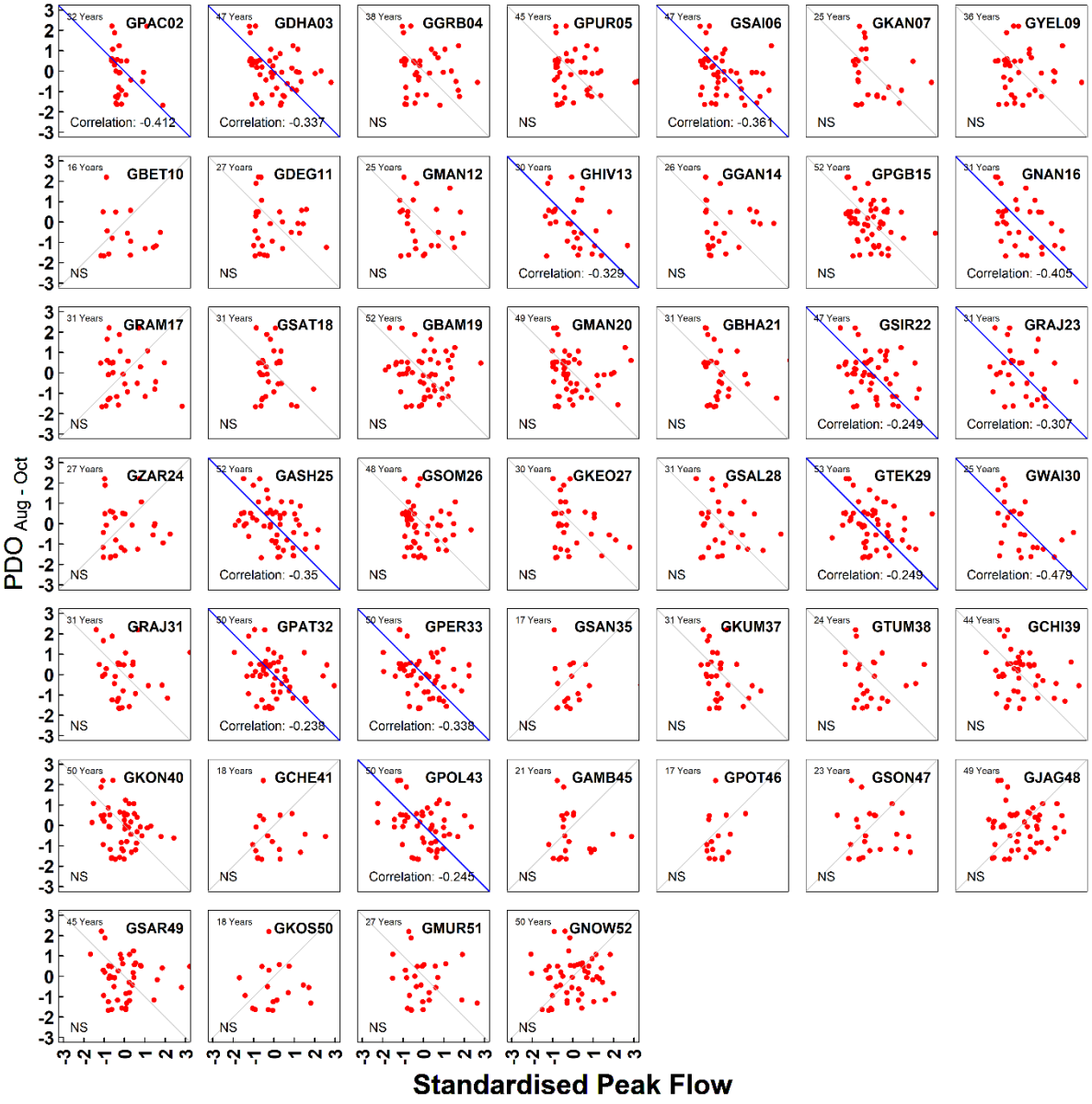

Figure 5. Rank-based Spearman correlations between August – October averaged Pacific Decadal Oscillation (PDO) indices and standardized annual peak flows in the selected gauges of Godavari River basin. Statistically significant correlations are highlighted with a blue

colored 1:1 line and the strength of correlation is given in the bottom right corner. Station code is indicated in the top right corner and the length of data used is given in the top left corner.

In contrast to the Godavari River basin, annual peak streamflow in the Narmada watershed did not show as many statistically significant correlations with PDO, Figure 6. Only two stations showed statistically significant but contradicting correlations. Although the annul peak flows in the streamflow gauge at Bamni Nanjar (Stn ID: NBAM04) show positive correlation with PDO, indicating that high magnitude floods at this station is more common during the positive phase of PDO, the data available at this station is only 17 years and so this correlation could be questionable. In contrast, the annual floods at the other station Chandwada (Stn ID: NCHA18) show a negative correlation concurring with the earlier observed the correlation with ISMR.

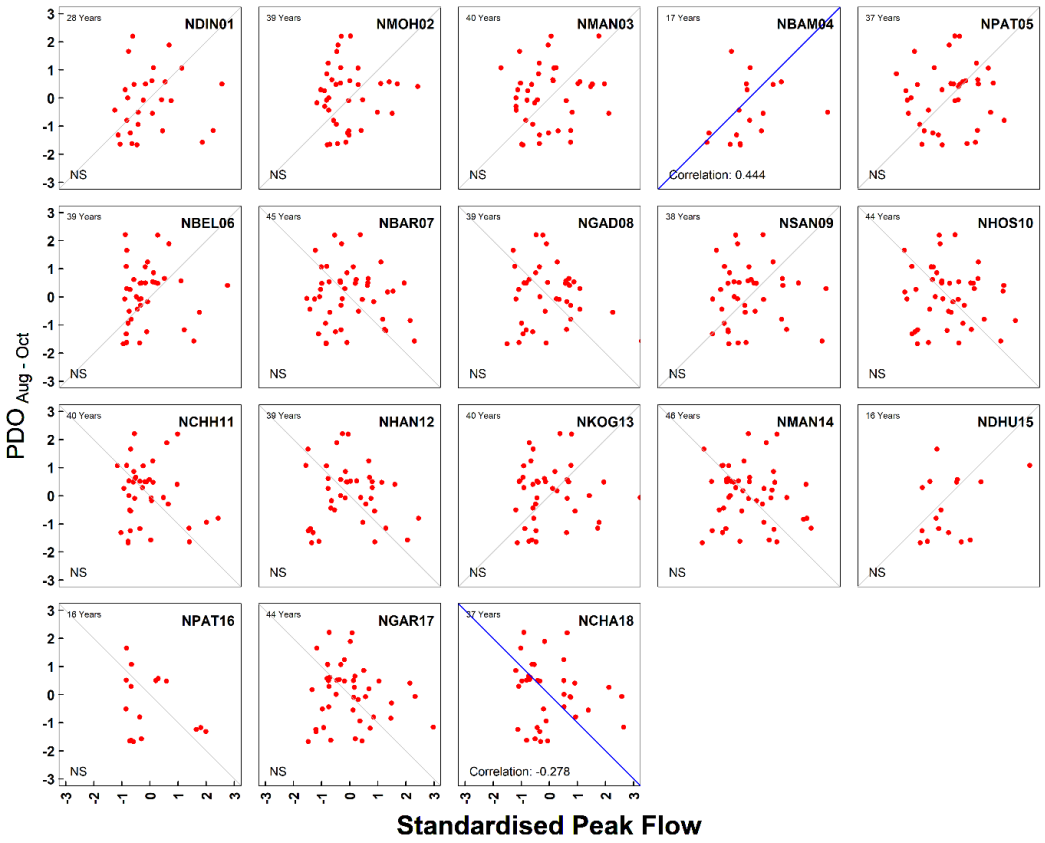

Figure 6. Rank-based Spearman correlations between August – October averaged Pacific Decadal Oscillation (PDO) indices and standardized annual peak flows in the selected gauges of Narmada River basin. Statistically significant correlations are highlighted with a blue colored 1:1 line and the strength of correlation is given in the bottom right corner. Station code is indicated in the top right corner and the length of data used is given in the top left corner.

$$Q_{std,\ i} = \frac{(Q_i - \bar{Q})}{(Q_{sd})} \qquad \text{…. Equation 1}$$

Where, $Q_{std,\ i}$ is the standardized annual peak streamflow for the year 'i', Q_i is the annual peak streamflow for the year 'i', $\bar{Q}$ is the mean of the annual peak flow series, and Q_{sd} is the standard deviation of the annual peak flow series.

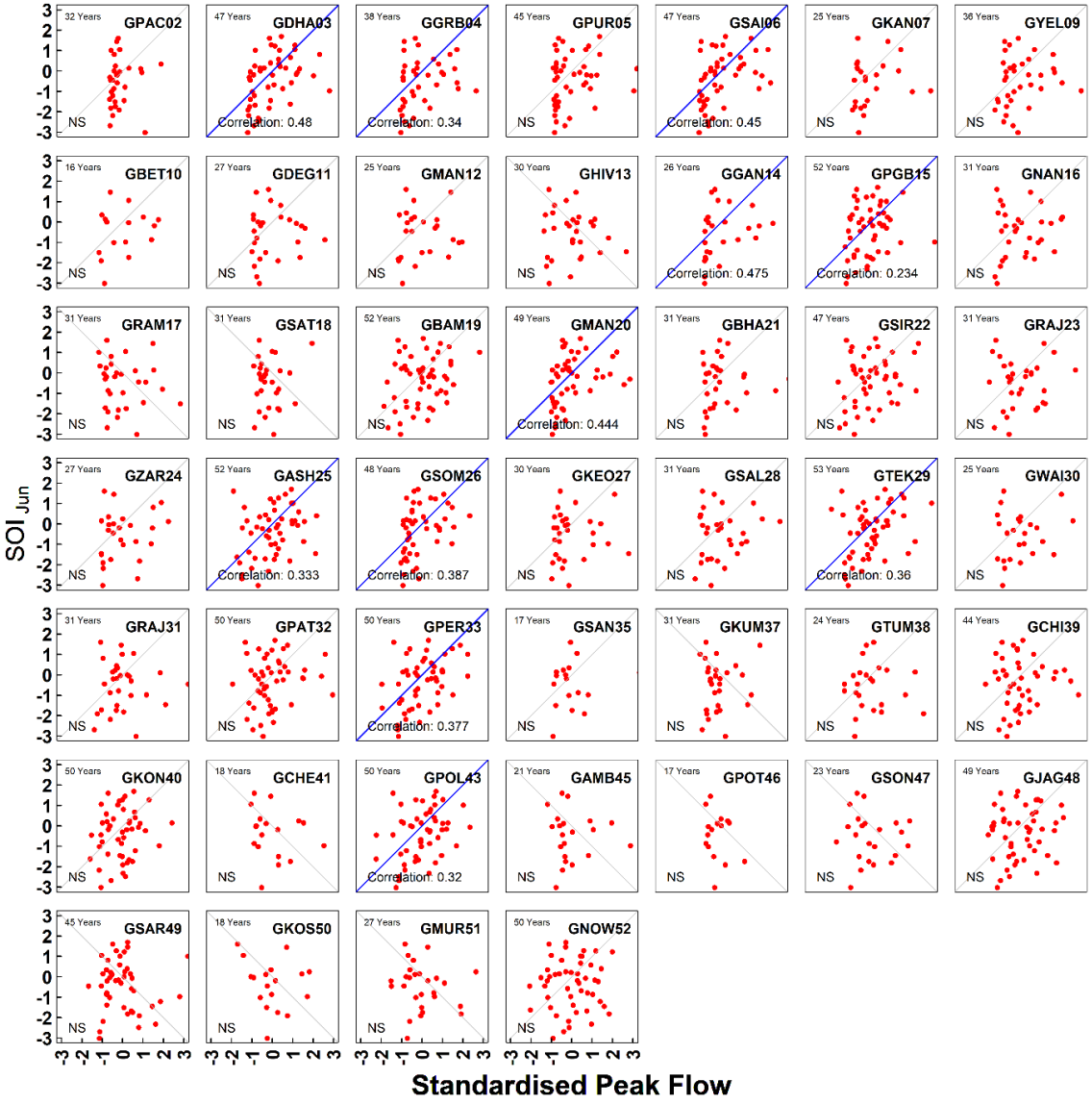

Figure 7. Rank-based Spearman correlations between June monthly Southern Oscillation Index (SOI) and standardized annual peak flows in the selected gauges of Godavari River basin. Statistically significant correlations are highlighted with a blue colored 1:1 line and the strength of correlation is given in the bottom right corner. Station code is indicated in the top right corner and the length of data used is given in the top left corner.

The influence of ENSO on annual floods is also evaluated using rank-based Spearman's correlations. Figure 7 presents the correlations with SOI, which is significantly correlated in 11 gauges across Godavari Basin. Annual floods are positively correlated at these sites and these results concur with the earlier observations that higher magnitude flood are common during La Niña episodes (SOI > 0.05). The statistically significant correlations indicate that as much as 48% variability in annual floods at these gauges can be explained by ENSO pattern.

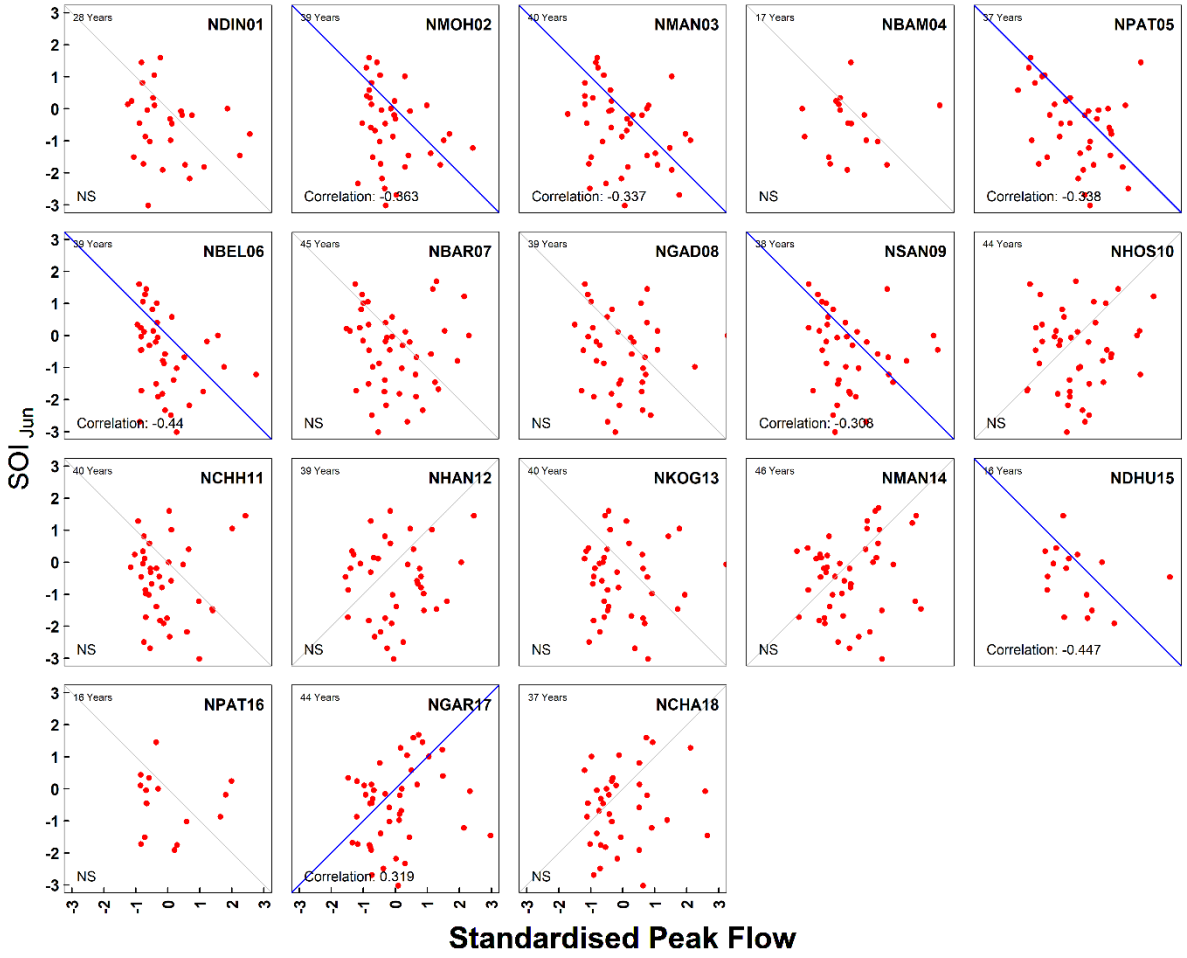

Figure 8. Rank-based Spearman correlations between June monthly Southern Oscillation Index (SOI) and standardized annual peak flows in the selected gauges of Narmada River basin. Statistically significant correlations are highlighted with a blue colored 1:1 line and the strength of correlation is given in the bottom right corner. Station code is indicated in the top right corner and the length of data used is given in the top left corner.

Figure 8 presents the correlations between annual floods in the gauges of Narmada River basin. In 7 of the gauging sites, the correlations are statistically significant, but indicate negative correlation at 6 gauging sites. These correlations indicate that the higher magnitude

floods at these locations are more common during the El Niño episodes of ENSO. These correlations do not agree with the earlier established observation that the El Niño episodes produce dry years. These negative correlations are as strong as -0.45, indicating that the 45% of variability in the annual floods at these stations can be explained by SOI. The gauging site at Garudeshwar (Stn ID: NGAR17) show statistically significant and positive correlation (Spearman's $\rho = 0.32$).

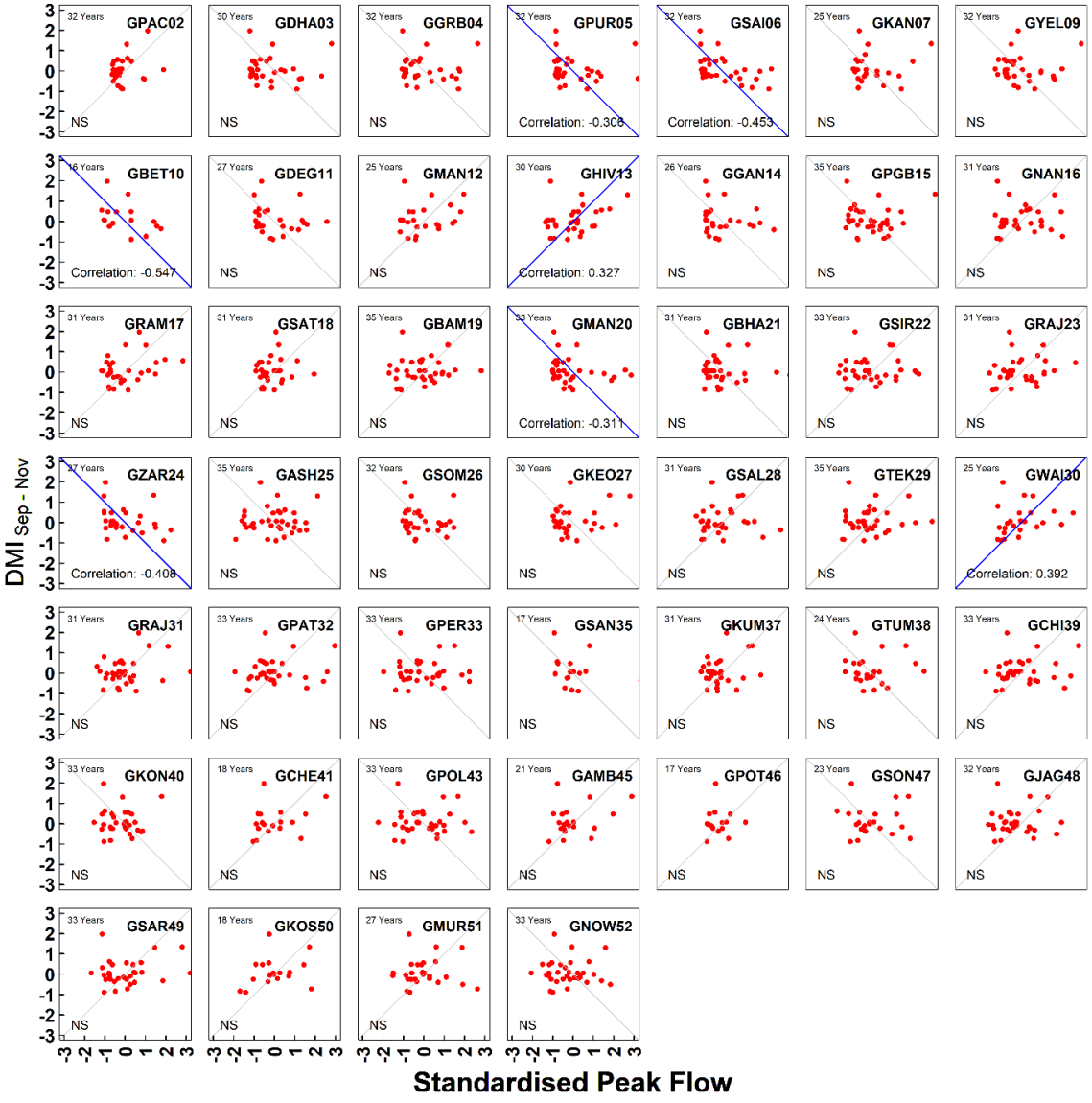

Figure 9. Rank-based Spearman correlations between September – November averaged Dipole Mode Index (DMI) and standardized annual peak flows in the selected gauges of Godavari River basin. Statistically significant correlations are highlighted with a blue colored 1:1 line and the strength of correlation is given in the bottom right corner. Station code is indicated in the top right corner and the length of data used is given in the top left corner.

Contradictory to the correlations between annual floods and PDO or ENSO, annual floods in Godavari basin do not show promising correlations with IOD, Figure 9. Seven gauges out of total 46 gauges show statistically significant correlations, but the correlations are not consistent. Among these, 2 gauges show positive and 5 gauges show negative correlations. And correlations with annual floods in the gauging sites across Narmada River basin do now show any statistically significant correlations with IOD, Figure 10.

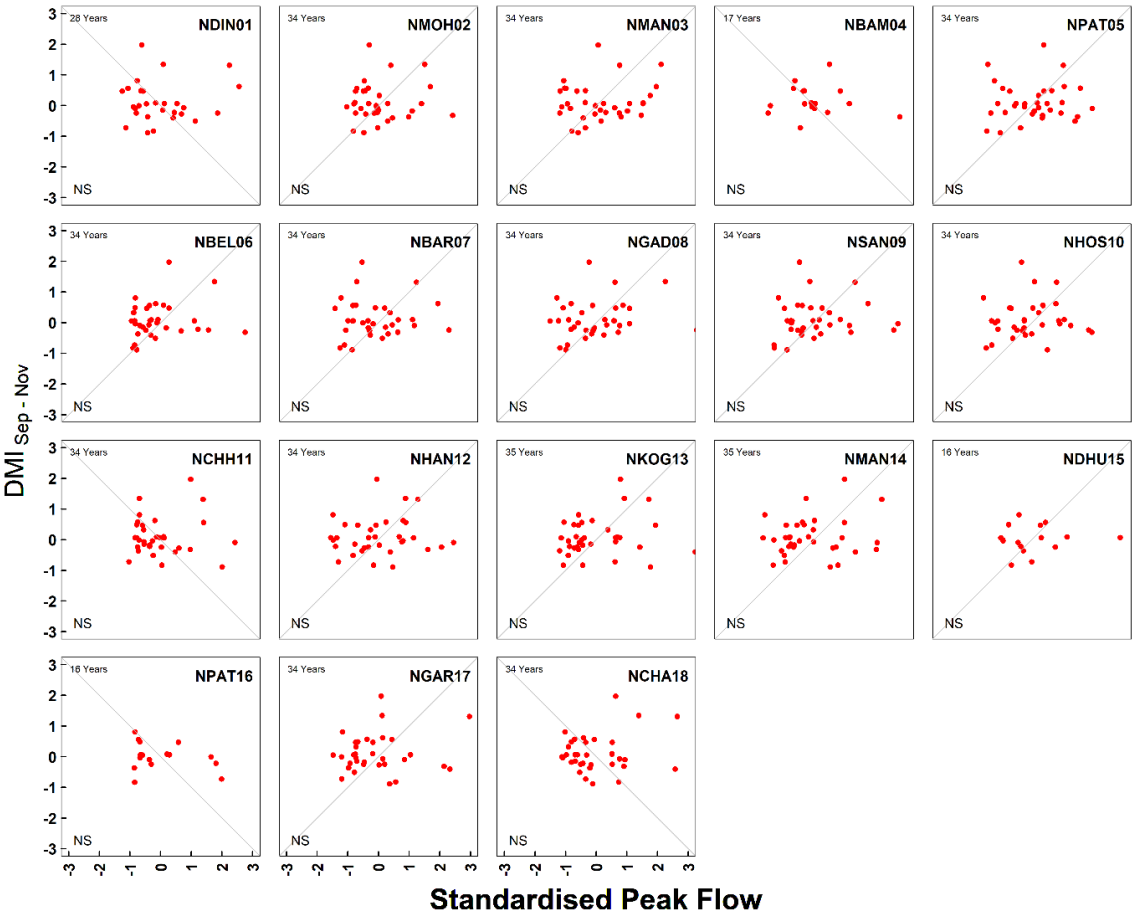

Figure 10. Rank-based Spearman correlations between September – November averaged Dipole Mode Index (DMI) and standardized annual peak flows in the selected gauges of Narmada River basin. Statistically significant correlations are highlighted with a blue colored 1:1 line and the strength of correlation is given in the bottom right corner. Station code is indicated in the top right corner and the length of data used is given in the top left corner.

Quantile-Quantile (Q-Q) Plot Analysis: The Q-Q plots also present evidence that PDO phase has a clear impact on annual peak flow magnitudes in Godavari River basin. Figure 11 shows the Q-Q plots for 46 gauges from across Godavari River basin. These Q-Q plots confirm that

it is unlikely that the annual peak flows are identically distributed regardless of the PDO phase since there are few gauges where the quantiles fall along the 1:1 line. The Q-Q plots demonstrate that higher magnitude floods are typically more common during the negative phase of PDO, since the flood quantiles largely appear above the 1:1 line. The permutation tests show that this is a significant result ($p < 0.1$) for 25 of the 46 records, i.e. more than 50% of the gauges indicate that the higher magnitude floods occurred during negative PDO phase.

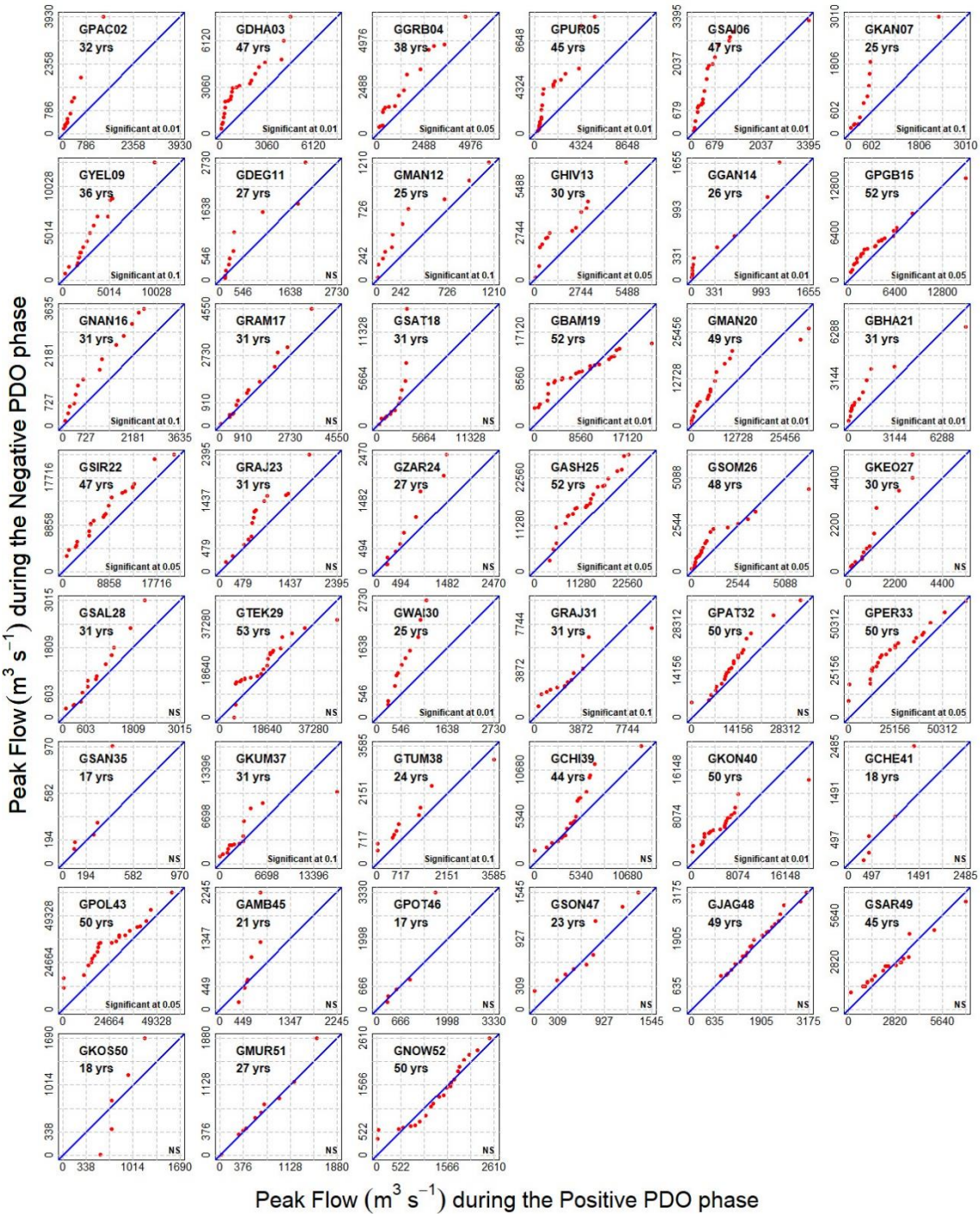

Figure 11. Quantile-Quantile plots based on annual peak flows (m^3/sec) stratified according Pacific Decadal Oscillations (PDO) phase for the 46 streamflow gauges in Godavari River basin. Shown in blue are the 1:1 lines. The stations codes are shown in the upper left hand corners, together with record length. Shown in the lower right corner are the statistical significance levels of the permutations test. NS indicated not significant.

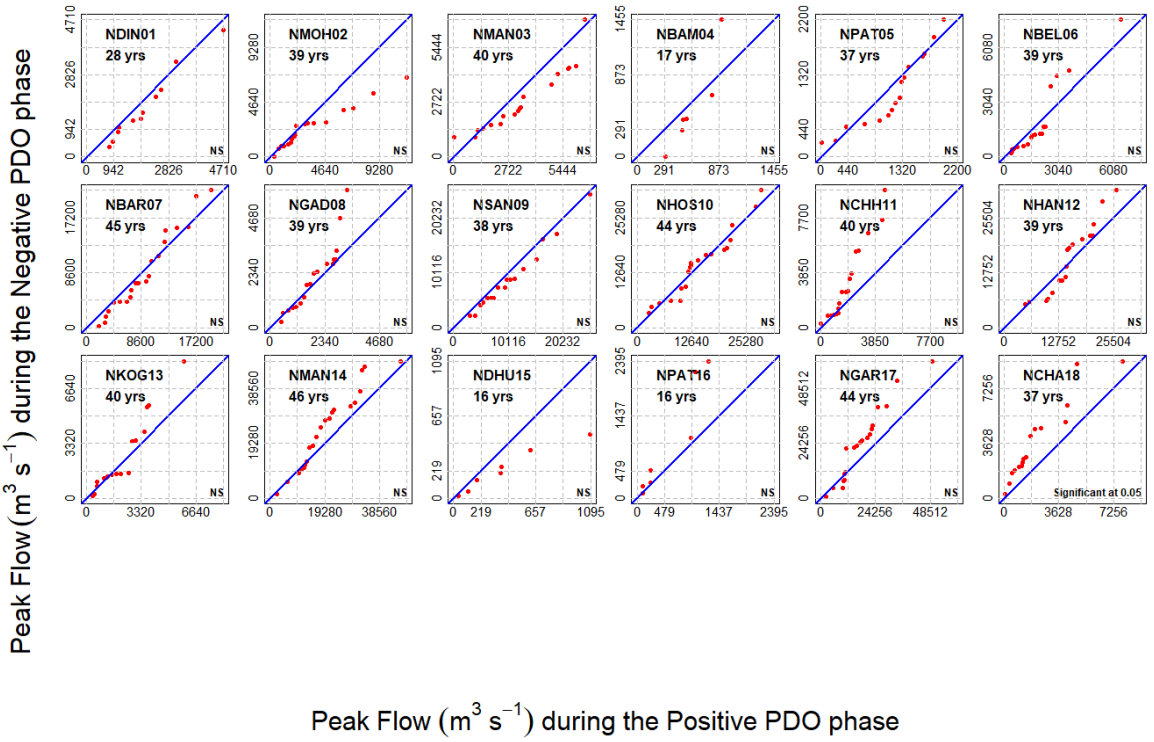

Figure 12. Quantile-Quantile plots based on annual peak flows (m^3/sec) stratified according Pacific Decadal Oscillations (PDO) phase for the 46 streamflow gauges in Narmada River basin. Shown in blue are the 1:1 lines. The stations codes are shown in the upper left hand corners, together with record length. Shown in the lower right corner are the statistical significance levels of the permutations test. NS indicated not significant.

Unlike the relationships observed in the gauges of Godavari River basin, the Q-Q plots constructed for the gauges of Narmada River basin fail to capture the effect of PDO on annual peaks, except for one gauge, Figure 12. The annual peak flows at the gauging site Chandwada (Stn ID: NCHA18) capture the PDO signal (statistically significant Q-Q plot) indicating that the higher magnitude floods are more common in the negative phase of PDO agreeing with the earlier observations made. Although the Q-Q plots of few other gauges visually indicate that higher magnitude flows are common in negative PDO phase (NMAN14, NCHH11, & NGAR17), they are not statistically significant. A few other gauging stations indicate an

inverse relationship, i.e. higher magnitude floods are common during positive phase of PDO (NMOH02, NMAN03, & NDHU15), although statistically insignificant. These inverse relationships can be explained by the inverse relationships observed between ISMR and PDO, evident in the earlier studies (e.g. Krishnamurthy & Krishnamurthy, 2013a), Figure A1.

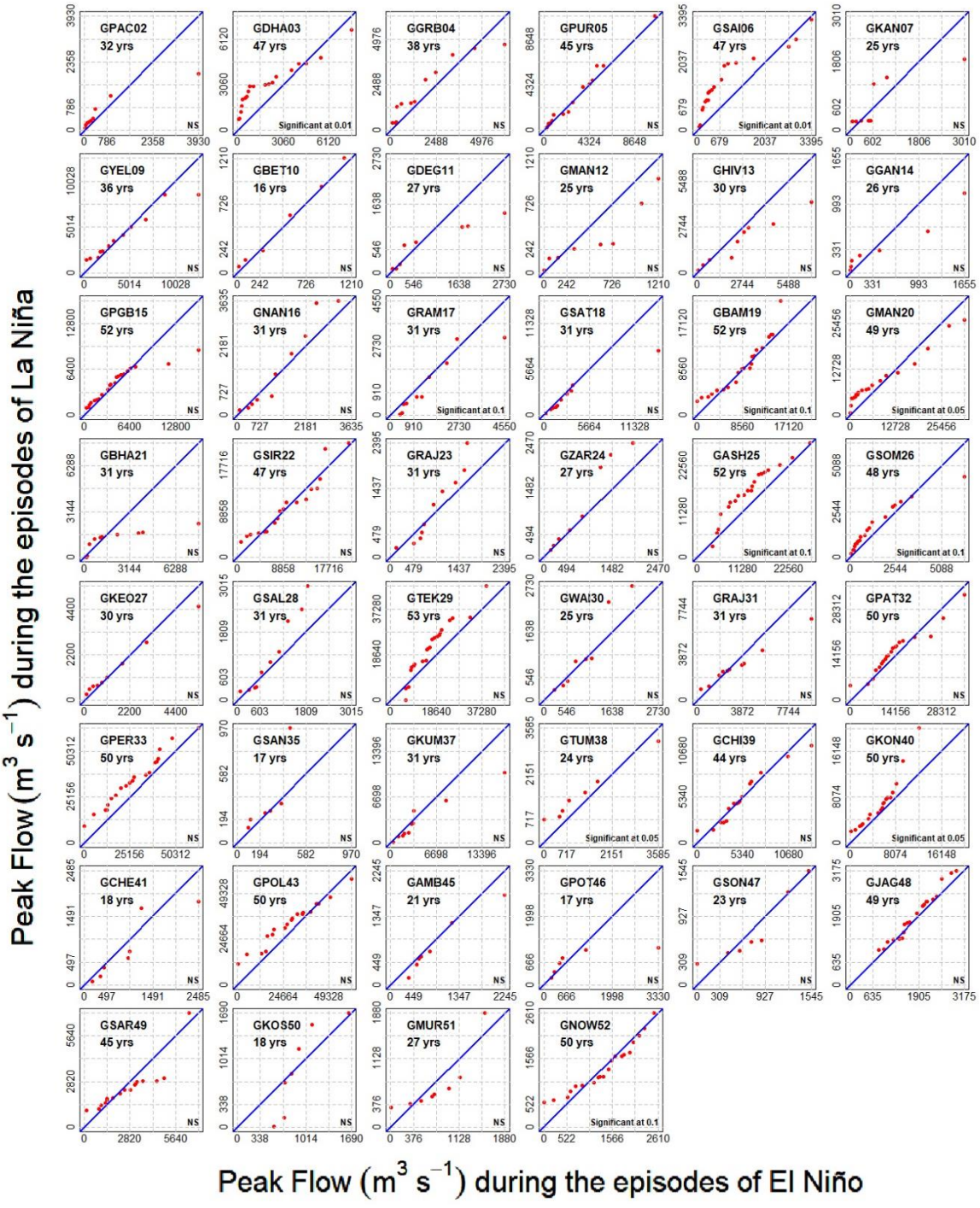

Figure 13. Quantile-Quantile plots based on annual peak flows (m^3/sec) stratified according to El Niño and La Niña episodes for the 46 streamflow gauges in Godavari River basin. Shown

in blue are the 1:1 lines. The stations codes are shown in the upper left hand corners, together with record length. Shown in the lower right corner are the statistical significance levels of the permutations test. NS indicated not significant.

The Q-Q plots were also constructed to evaluate the relationships between the ENSO and annual peak flows in all the selected gauging stations, Figures 13 & 14. In Godavari River basin, 10 stations out of 10 out of 46 stations (22%) indicate that higher floods are common during the La Niña episodes of ENSO, concurring with the earlier identified relationships between ISMR and ENSO. Although the relationships are not statistically significant the some of the other stations, the Q-Q plots indicate higher magnitude floods during the La Niña episodes. In contrast, 11 out of 18 gauging stations (61%) in Narmada River Basin indicate that higher magnitude floods are more common during the El Niño episodes of ENSO, Figure 14. Of these, 7 gauging stations show statistically significant relations. These inverse relationships can again be explained by the inverse relationships between ISMR and ENSO along the central part of India, Figure A1.

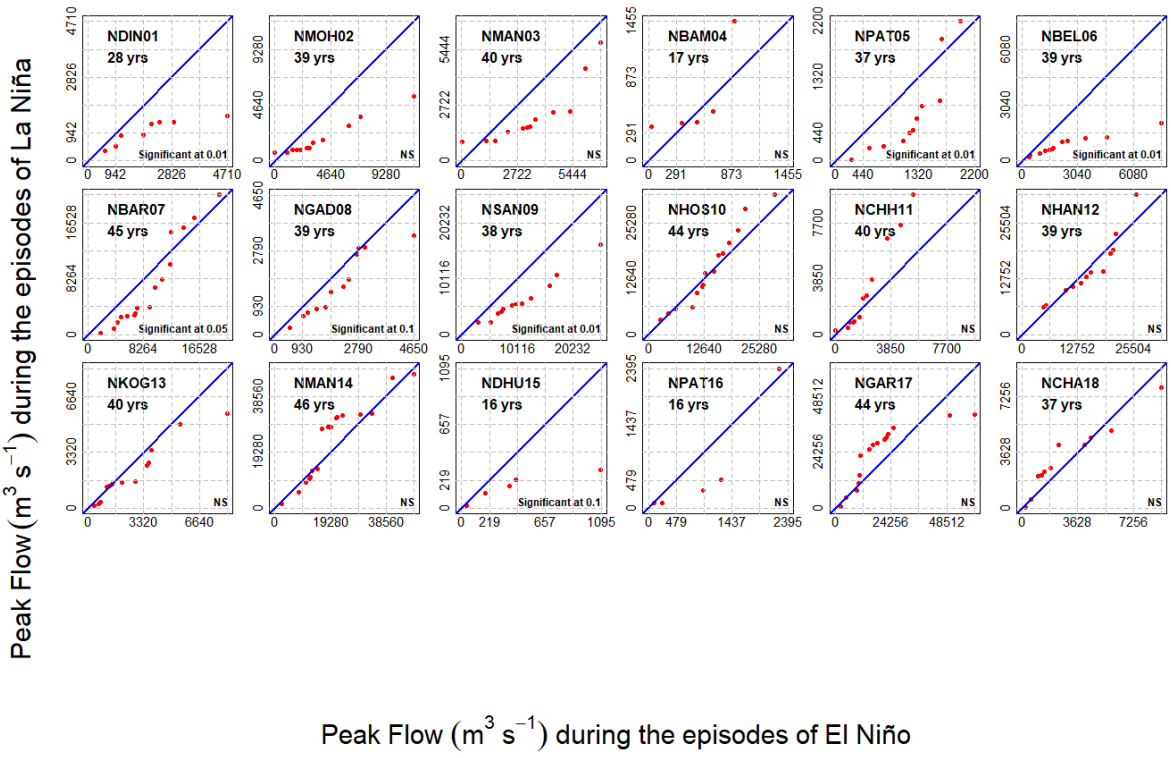

Figure 14. Quantile-Quantile plots based on annual peak flows (m^3/sec) stratified according to El Niño and La Niña episodes for the 46 streamflow gauges in Narmada River basin. Shown in blue are the 1:1 lines. The stations codes are shown in the upper left hand corners, together

with record length. Shown in the lower right corner are the statistical significance levels of the permutations test. NS indicated not significant.

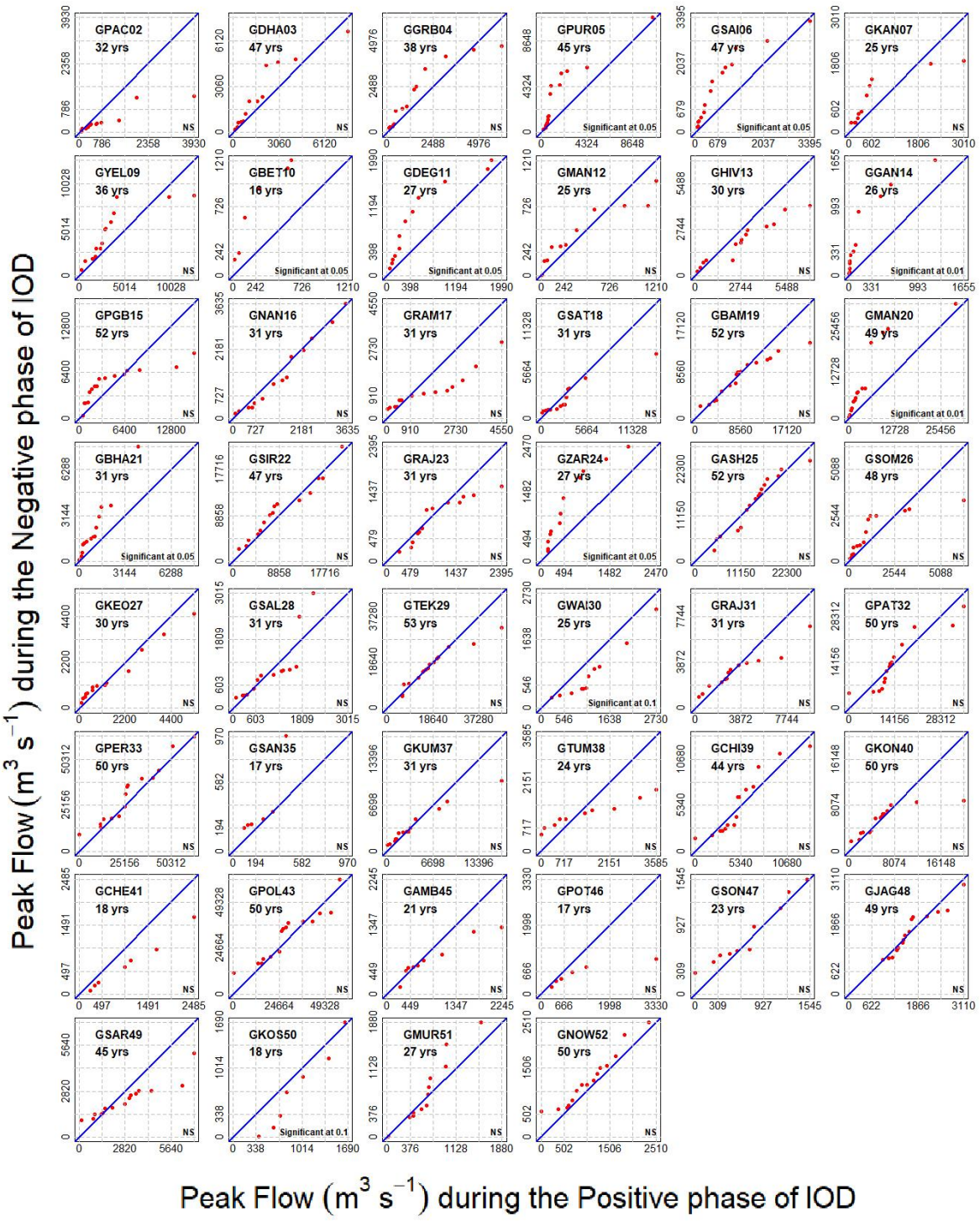

Figure 15. Quantile-Quantile plots based on annual peak flows (m^3/sec) stratified according to positive and negative phases of Indian Ocean Dipole (IOD) for the 46 streamflow gauges in Godavari River basin. Shown in blue are the 1:1 lines. The stations codes are shown in the

upper left hand corners, together with record length. Shown in the lower right corner are the statistical significance levels of the permutations test. NS indicated not significant.

Figures 15 and 16 present the Q-Q plots evaluating the impacts of IOD on annual peak flows in both Godavari and Narmada River basins. 10 out of 46 gauging stations (22%) in Godavari River basin show statistically significant relationships. Of these, Q-Q plots of 8 stations indicate that higher magnitude floods are more common in the negative phase of IOD, whereas at the 2 other stations the Q-Q plots indicate that the higher magnitude floods are common in the positive phase of IOD. In contrast, none of the gauging stations in Narmada seem to be impacted by the phase of IOD. While the impact of IOD on ISMR is felt across India to some extent, the relationship is strong and statistically significant mostly across the southern part of India (e.g. Li et al.,0 2017). So, only those gauging stations located along the southern part of the Godavari River basin show statistically significant relationship between IOD and Annual peak flows, whereas the same cannot be seen in the northern part of Godavari River basin and the Narmada River Basin.

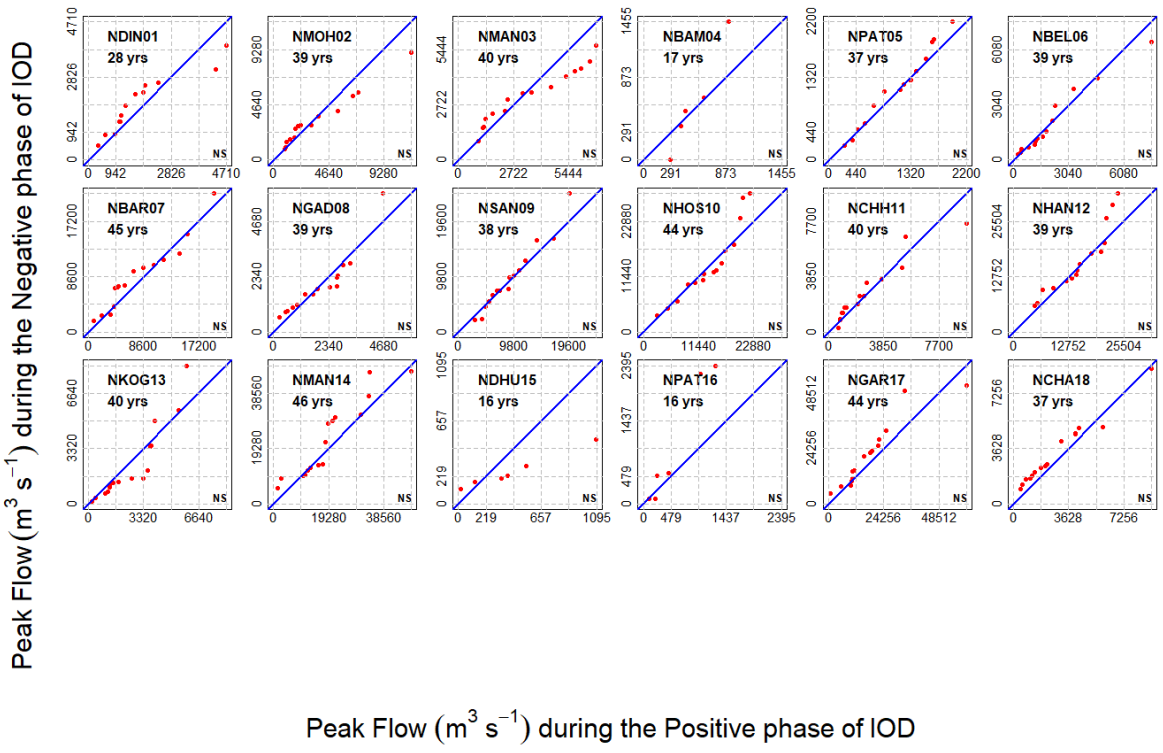

Figure 16. Quantile-Quantile plots based on annual peak flows (m^3/sec) stratified according to positive and negative phases of Indian Ocean Dipole (IOD) for the 46 streamflow gauges in Narmada River basin. Shown in blue are the 1:1 lines. The stations codes are shown in the

upper left hand corners, together with record length. Shown in the lower right corner are the statistical significance levels of the permutations test. NS indicated not significant.

Flood Frequency Curves: Flood frequency analysis provide further evidence that it is unlikely that the annual peak flows are independent and identically distributed regardless of the phases of PDO, ENSO, or IOD.

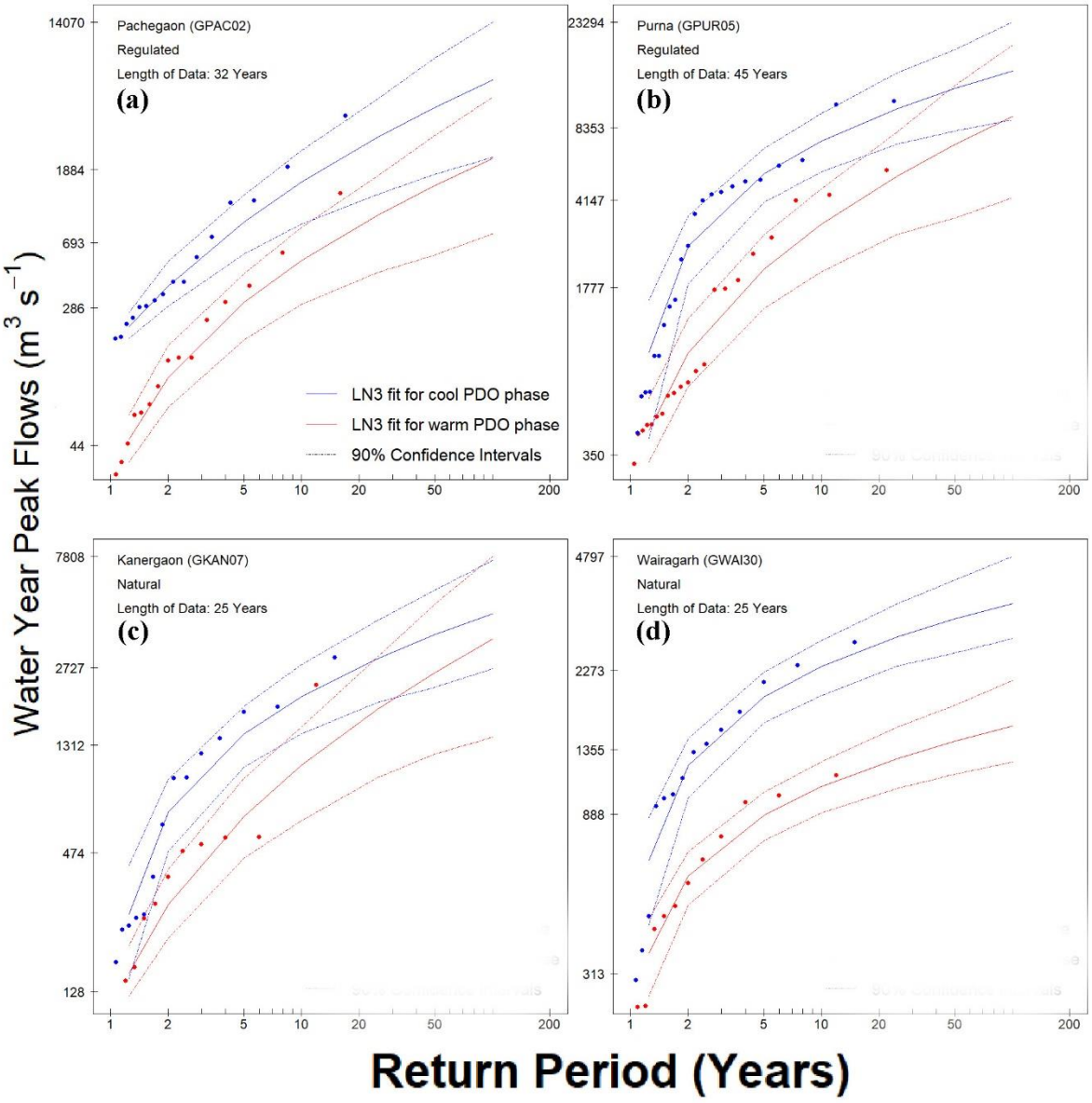

Figure 17. 3-Parameter Lognormal (LN3) flood frequency curves (solid lines) and their 90% confidence intervals (dashed lines) for the annual peak flows in selected gauges of Godavari River Basin, stratified according to negative (Aug–Oct averaged PDO index < −0.05) and

positive (Aug–Oct averaged PDO index > 0.05) PDO phases of the Pacific Decadal Oscillation (PDO). (a) Pachegaon, (b) Purna, (c) Kanergaon, and (d) Wairagarh.

Figure 17 presents the flood frequency curves the for 4 gauging stations spread across Godavari River basin, the curves fit to the annual floods stratified based on the positive (red curves) and negative (blue curves) phases of PDO. Two of the stations (a & b) are regulated and the other 2 stations (c & d) are located on the naturally flowing streams. All the four stations clearly indicate that the hydrological response of the watershed in both the phases of PDO is distinctly different. The flood frequency curves (red & blue) separate clearly indicating that the annual floods are not identically distributed. Also, there is a clear evidence that the higher magnitude floods are more common during the negative phase of PDO. Not all the gauging sites show such a relationship (clear separation of flood frequency curves), but majority of the gauging stations analysed show a clear indication of the impact of PDO on annual floods. Majority of the stations show clear separation of the flood frequency curves for the higher magnitude floods. Irrespective of whether the station is on a naturally flowing or on a regulated stream, the flood frequency plots show clear signal of PDO.

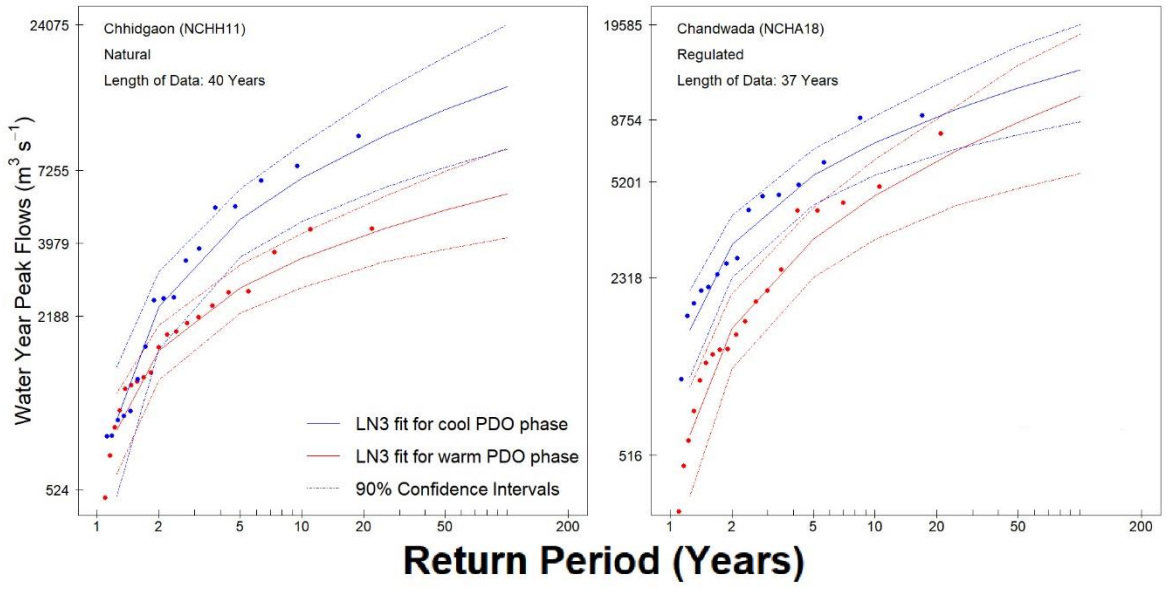

Figure 18. 3-Parameter Lognormal (LN3) flood frequency curves (solid lines) and their 90% confidence intervals (dashed lines) for the annual peak flows in selected gauges of Narmada River Basin, stratified according to negative (Aug–Oct averaged PDO index < -0.05) and positive (Aug–Oct averaged PDO index > 0.05) PDO phases of the Pacific Decadal Oscillation (PDO). (a) Chhidgaon, (b) Chandwada.

The gauging stations from Narmada River basin also indicate that higher magnitude floods are more common in the negative phase of PDO, when compared to the positive PDO phase, Figure 18. Irrespective of the regulations on the stream, annual floods collected from selected gauging sites show a clear signal of PDO. Similar to what has been observed in the annual floods from the stations of Godavari River basin, not all the gauging sites show the impact of PDO on annual floods and flood frequency, but such a relationship can be seen in the flood frequency curves of all selected stations of Narmada River basin.

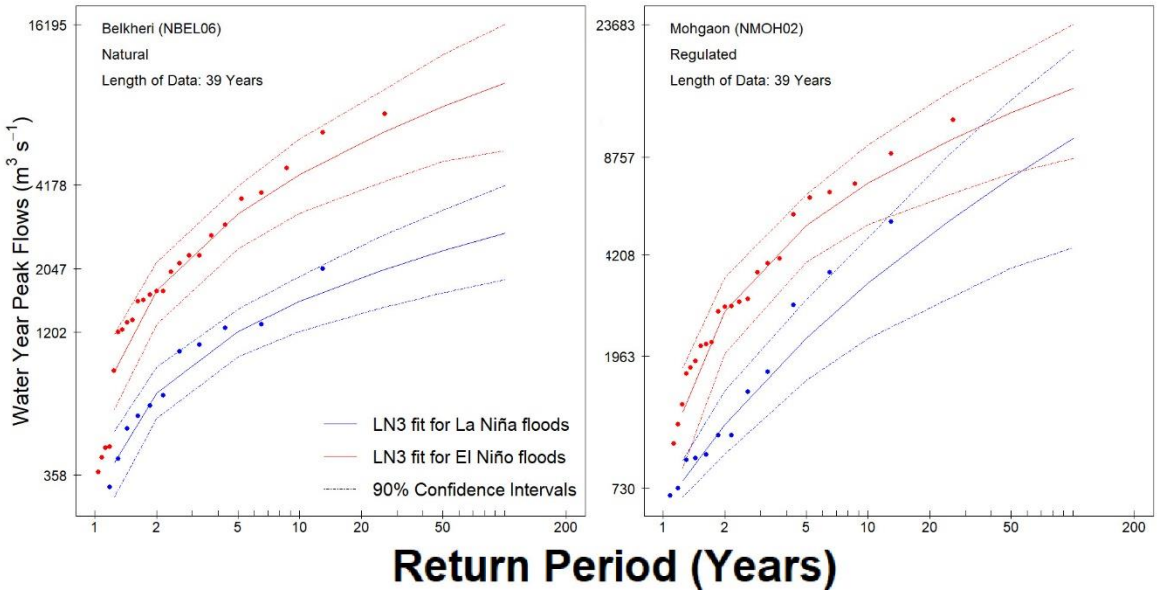

Figure 19. 3-Parameter Lognormal (LN3) flood frequency curves (solid lines) and their 90% confidence intervals (dashed lines) for the annual peak flows in selected gauges of Narmada River Basin, stratified according to El Niño (SOI < -0.05) and La Niña (SOI index > 0.05) episodes of El Niño-Southern Oscillation (ENSO) pattern. (a) Belkheri, (b) Mohgaon.

The impact of ENSO on annual floods in the selected gauging stations of Godavari River basin is not clearly seen in the flood frequency curves (results not presented). Although, a few stations show a separating flood frequency curves, the separation is not distinct enough to prove the influence of ENSO and flood frequency. A few stations show that the frequency and magnitude of floods is higher in the negative PDO phase, whereas few other stations depict an inverse relationship, although not very distinct. In contrast, the effect of ENSO on flood frequency and magnitude in selected gauging stations of Narmada River basin indicate that the frequency and magnitude of floods is relatively higher during the El Niño episodes when compared to those during the La Niña episodes of ENSO, Figure 19. At a gauging station on

the naturally flowing stream, there is a clear separation of flood frequency curves of annual floods during El Niño and La Niña episodes of ENSO, Figure 19(a). This indicates that the flood characteristics are distinctly different with respect to the phase of ENSO.

Flood Ratio Analysis: Even though only a few stations show clear separation of the flood frequency curves stratified based on the phase of low-frequency oscillations, flood ration analysis is adopted to evaluate the regional impact of these oscillations. Using the flood quantiles estimated through flood frequency analysis, flood ratio is computed for each gauging stations at several return periods. Figures 20 – 25 shows histograms of the flood ratios for all the selections gauging stations of Godavari River basin (Figures 20, 22, 24) and Narmada River basin (Figures 21, 23, 25). If the annual floods in the selected gauging stations are independent and identically distributed, at least 50% of the selected gauging stations would have flood ratio (FR) ≤ 1.

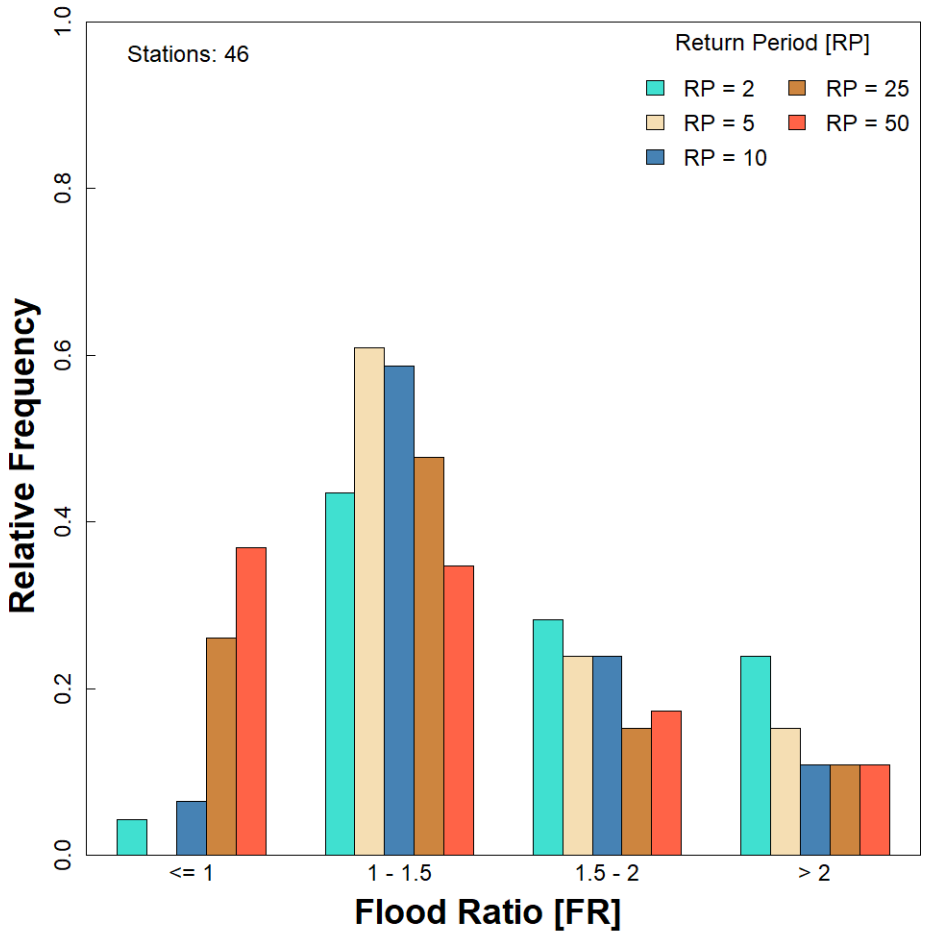

Figure 20. Histogram of flood ratios (FR) for return periods between 2 and 50 years for the 46 streamflow gauging stations in Godavari River Basin. FR is the ratio of flood quantiles in

negative and positive phases of PDO, extracted after fitting the stratified annual peak flow data to a 3-parameter lognormal distribution.

Figure 20 presents the histogram of flood ratios (at various return periods) of 46 gauging stations spread across Godavari River basin to show the impact of PDO. This figure clearly indicates that the flood ratio is more than 1 in at least 50% of the gauging stations for all the return periods. For at least 10% of the selected gauging stations, this ratio is higher than 2, which is a very strong evidence of the impact of PDO. Figure 21 presents the histogram of floods rations of 18 flow gauging stations spread across Narmada River Basin to show the impact of PDO. This figure indicates that the floods of higher frequency (i.e. RP = 2 or 5) can be assumed to be independent and identically distributed, whereas the less frequent floods (i.e., RP = 10 or 25 or 50) are affected by PDO. At return periods 10, 25, and 50, flood ratio is much higher than 1 in more than 50% of the gauging stations, a clear evidence of teleconnection.

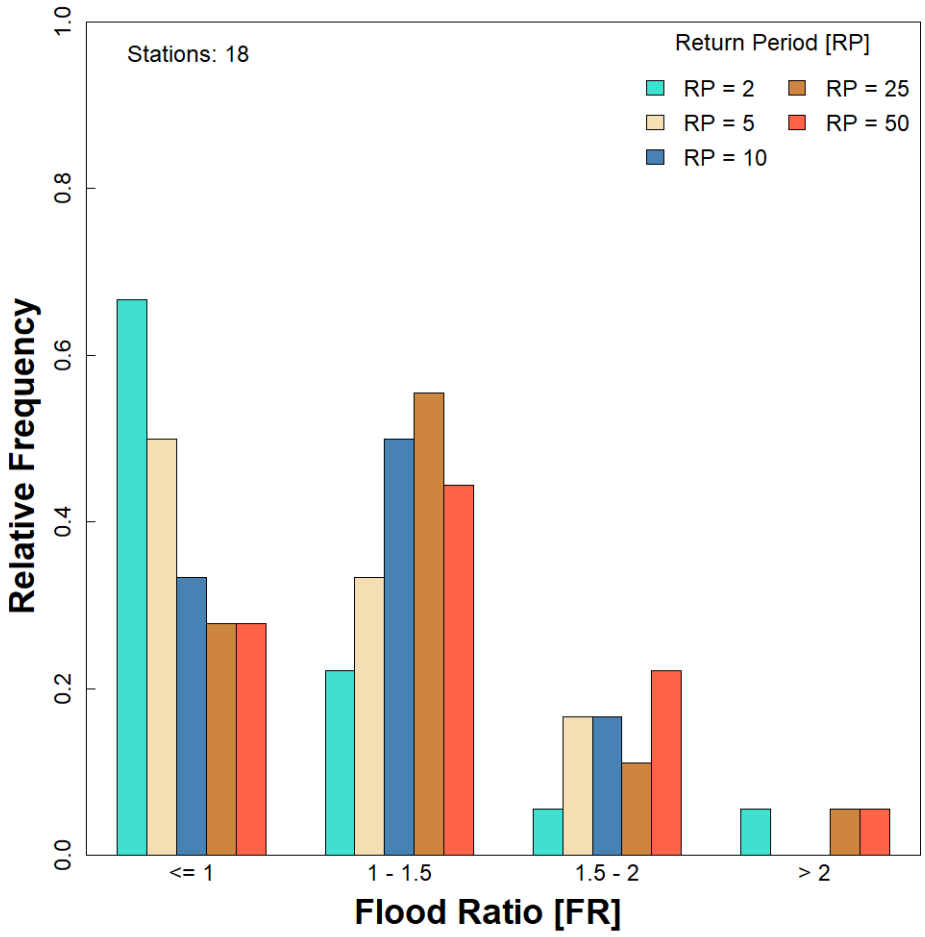

Figure 21. Histogram of flood ratios (FR) for return periods between 2 and 50 years for the 18 streamflow gauging stations in Narmada River Basin. FR is the ratio of flood quantiles in

negative and positive phases of PDO, extracted after fitting the stratified annual peak flow data to a 3-parameter lognormal distribution.

Figure 22 presents the histogram of flood ratios of all the selected gauging stations spread across Godavari River basin to show the impact of ENSO. This figure indicates that the annual floods at these stations can be assumed to be independent and identically distributed, because the flood ratio is less than 1 in nearly 50% of the stations and is more than 1 in the other half. Although the impact of ENSO is not evident here, its impact on annual floods was found in the analysis discussed in previous sections. In Narmada River basin, annual floods with higher frequency (i.e. RP = 2 or 5 or 10) are more common during the El Niño episodes of ENSO, because the FR < 1 in more than 50% of the stations analysed, Figure 23. In contrast, the lower frequency floods (i.e. RP = 25 or 50) can be assumed to be independent and identically distributed, because FR is ≤ 1 and > 1 in nearly 50% of the stations analysed.

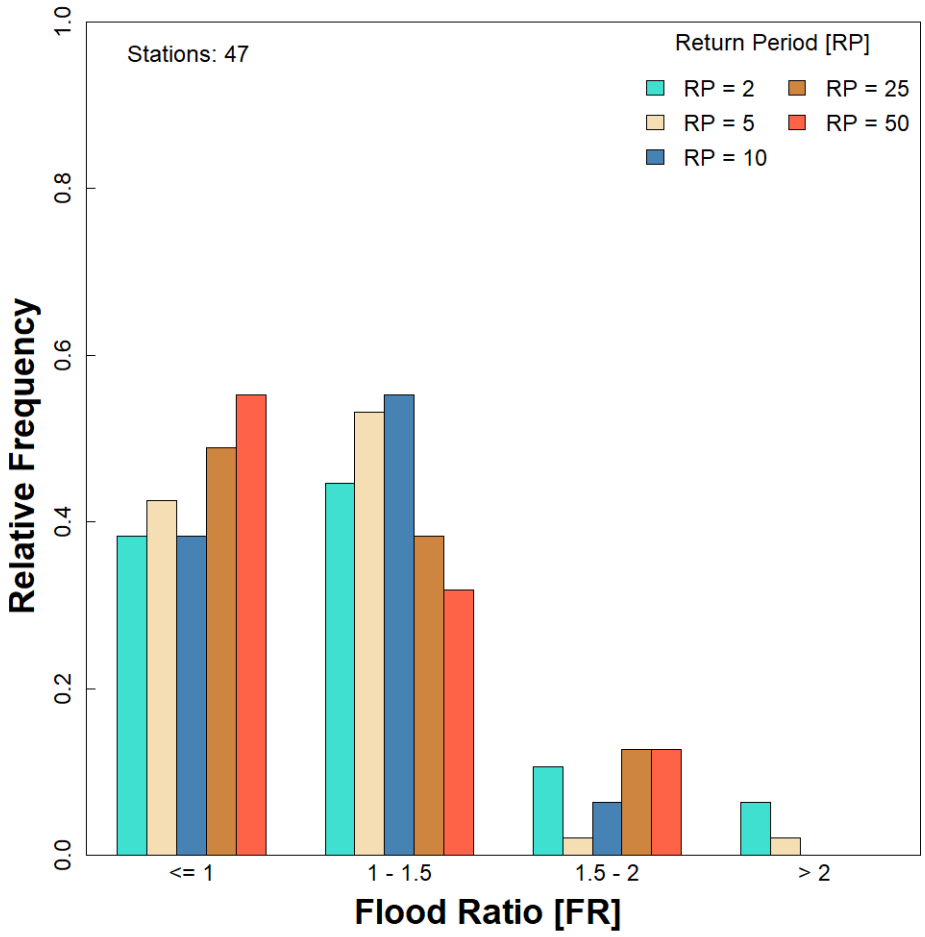

Figure 22. Histogram of flood ratios (FR) for return periods between 2 and 50 years for the 47 streamflow gauging stations in Godavari River Basin. FR is the ratio of flood quantiles in the

La Niña and El Niño episodes of ENSO pattern, extracted after fitting the stratified annual peak flow data to a 3-parameter lognormal distribution.

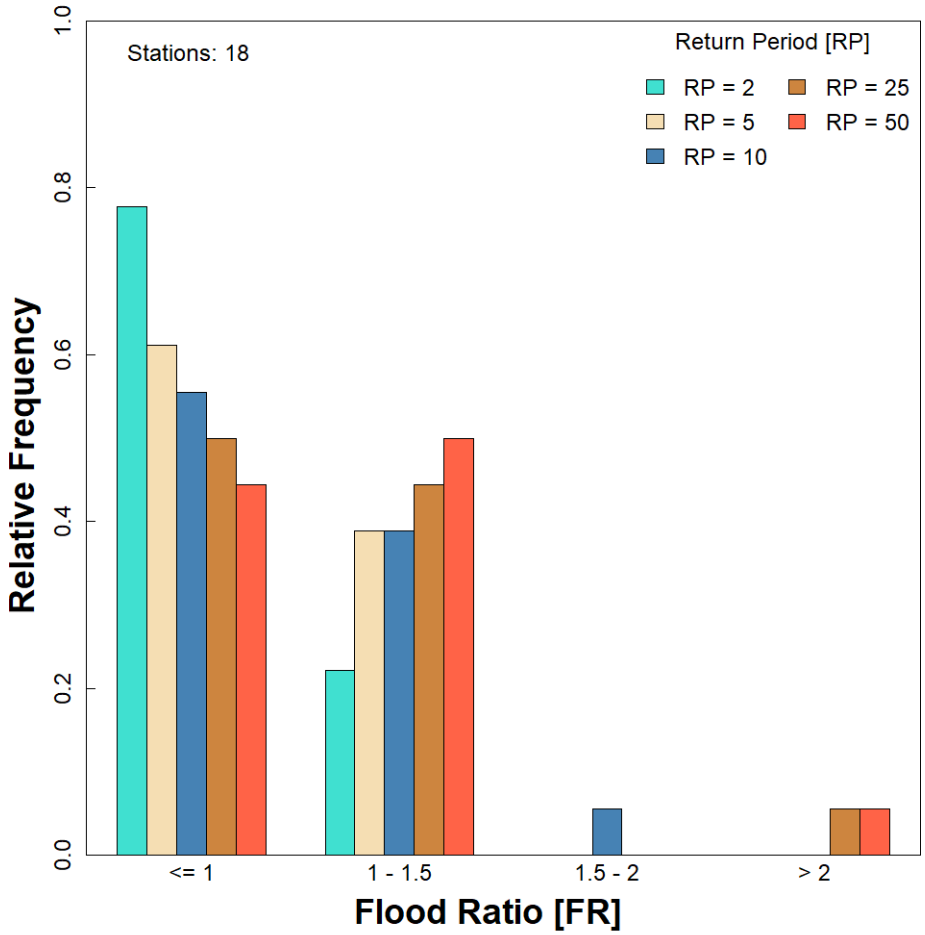

Figure 23. Histogram of flood ratios (FR) for return periods between 2 and 50 years for the 18 streamflow gauging stations in Narmada River Basin. FR is the ratio of flood quantiles in the La Niña and El Niño episodes of ENSO pattern, extracted after fitting the stratified annual peak flow data to a 3-parameter lognormal distribution.

The regional influence of IOD on annual floods is also analysed using flood ration approach. Figures 24 & 25 show the histogram of flood ratios in all the selected gauging stations of Godavari River and Narmada River basins. The effect of IOD on annual floods in Godavari River basin is not evident in this analysis, because approximately 50% of the gauging stations show FR $\leq$ 1 and the 50% of the stations have FR > 1. So it can be assumed that the annual floods in Godavari River basin are least affected by the phase of IOD and it can be assumed that the annuals floods are independent and identically distributed in this basin. However, floods with lower frequency (i.e. RP = 50) and higher frequency (i.e. RP = 2 or 5)

indicate that higher magnitude floods are marginally higher during positive phase (FR < 1 in nearly 60% of the stations) and negative phase (FR > 1 in nearly 60% of the stations) of IOD, Figure 24.

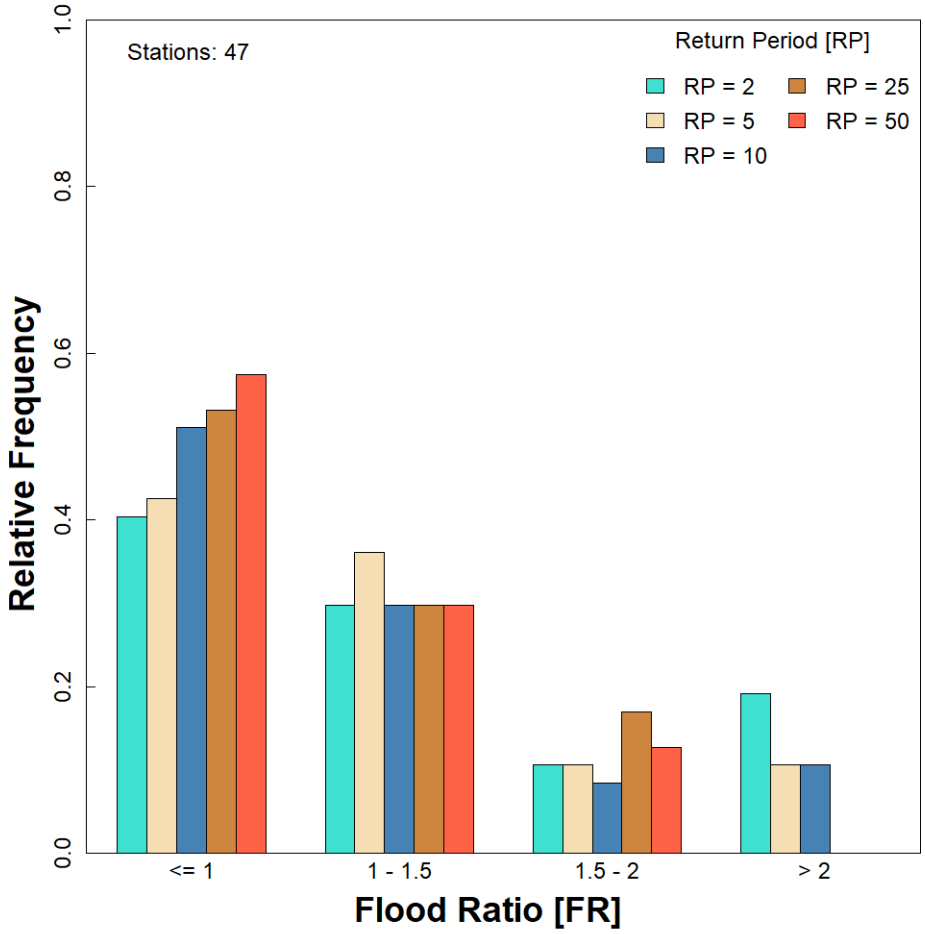

Figure 24. Histogram of flood ratios (FR) for return periods between 2 and 50 years for the 47 streamflow gauging stations in Godavari River Basin. FR is the ratio of flood quantiles in the Negative and positive phases of the IOD oscillation, extracted after fitting the stratified annual peak flow data to a 3-parameter lognormal distribution.

Figure 25 show the histogram of flood ratios of the selected gauging stations spread across Narmada River Basin. This indicates that frequently (RP = 2 or 5 or 10) occurring annual floods are more common during the negative phase of IOD, i.e. FR > 1 in more than 50% of the stations analysed. Although the effect of IOD on annual floods in Narmada Basin is not evident according to the flood frequency analysis, the flood ratio analysis indicate that the higher magnitude and most frequent floods may be expected during the negative phase of IOD. However, the less frequent floods are least influenced by the phase of IOD, because FR is

neither greater than 1 or less than 1 in more than 50% of the stations analysed. So, in Narmada River basin, less frequent floods may be assumed to be independent and identically distributed, whereas the high frequent floods are affected by the phase of PDO.

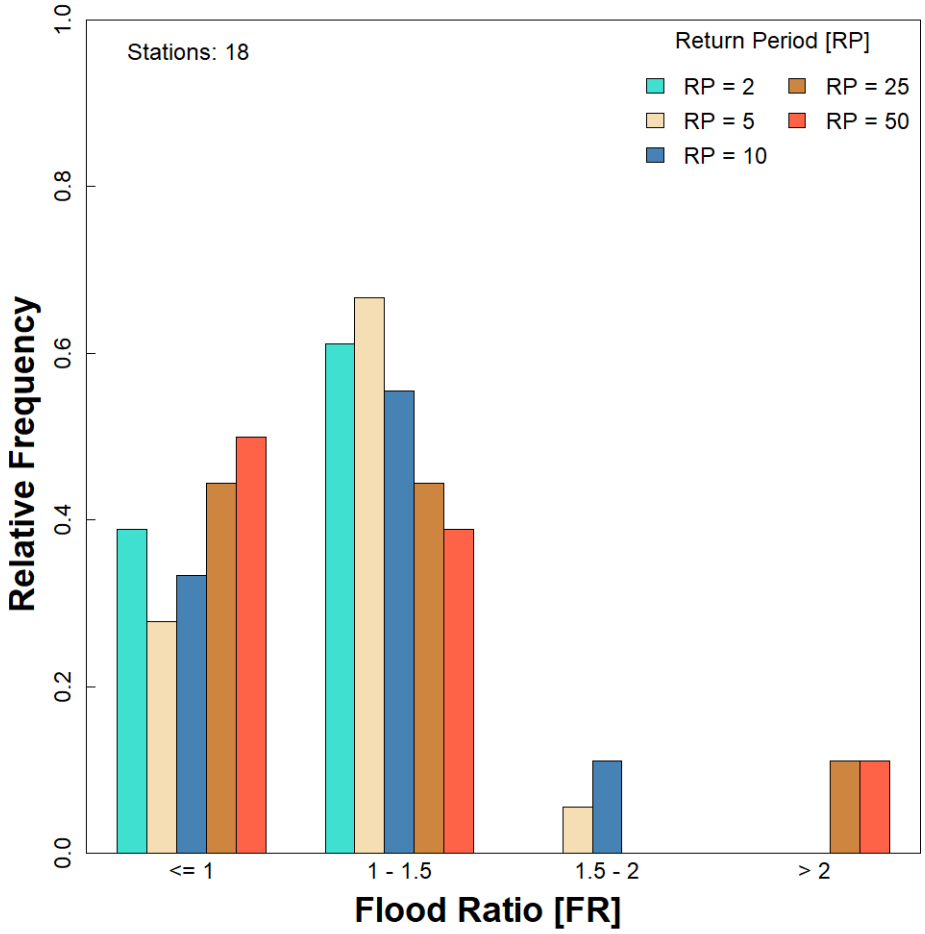

Figure 25. Histogram of flood ratios (FR) for return periods between 2 and 50 years for the 18 streamflow gauging stations in Narmada River Basin. FR is the ratio of flood quantiles in the Negative and positive phases of the IOD oscillation, extracted after fitting the stratified annual peak flow data to a 3-parameter lognormal distribution.

CONCLUSIONS

Return period or frequency of a flood event is one key information required for adequate planning and design of water resources infrastructure and for effective management of available water. Traditionally, such information is obtained from flood frequency analysis, which assumes that the annual peak flow series is independent and identically distributed. Almost all the flood frequency analysis done in India invokes the assumption of *i.i.d.* and this

study is aimed to evaluate its adequacy in making estimates of design flood. Results from this study highlight the potential inadequacy of *i.i.d.* assumption and these results are in agreement with the observations made by other researchers across the globe (e.g. Gurrapu et al., 2016; Barros et al., 2014; López and Francès, 2013; Stedinger and Griffis, 2008; 2011; Kwon et al., 2008). Therefore, the knowledge of the regional hydroclimate with regards to phases of the large-scale atmosphere-ocean oscillations should be considered prior to estimating design flood. Ignoring the multi-decadal variability of large-scale climate states could lead to flood risk underestimation, and under-design of key infrastructure. Overall, the results from this study reveal that the *i.i.d.* assumption is not tenable where the hydroclimatology is strongly influenced by the low-frequency atmosphere-ocean oscillations. This is a manifest in Godavari River basin and parts of Narmada River basin in India and other parts across the globe including western Canada, California and eastern Australia (e.g. this study; Gurrapu et al., 2016; Franks and Kuczera, 2002; Ward et al., 2014). The extent of this problem in other Indian watersheds remains to be explored. Any region with a strong teleconnection with the PDO, ENSO, or IOD may be subject to under- or overestimation of design flood and so, the phase of the teleconnections should be considered while estimating the design flood. Furthermore, the effect of other atmosphere-ocean oscillations, e.g. North Atlantic Oscillation (NAO), Arctic Oscillation (AO) and Atlantic Multi-Decadal Oscillation (AMO), on regional extreme hydrology needs to be explored.

BIBLIOGRAPHY

1. Andrews E D, Antweiler R C, Neiman P J, and Ralph F M. 2004. Influence of ENSO on Flood Frequency along the California Coast. *Journal of Climate* 17(2): 337-348. DOI: 10.1175/1520-0442(2004)017%3C0337:IOEOFF%3E2.0.CO;2.
2. Barros A P, Duan Y, Brun J, and Medina M A. 2014. Flood Non-stationarity in the SE and Mid-Atlantic Regions of the United States. *Journal of Hydrologic Engineering* **19 (10)**: 05014014. DOI: 10.1061/(ASCE)HE.1943-5584.0000955.
3. Bhattacharya S, and Das A. 2007. *Vulnerability to Drought, Cyclones, and Floods in India*. The BASIC Project Paper 9. Winrock International, India. 43 pp.
4. Bryant E. 2005. *Natural Hazards*. Cambridge: Cambridge University Press.
5. Clavet-Gaumont J, Huard D, Frigon A, Koeing K, Slota P, Rousseau A, Klien I, Thiémonge N, Houdré F, Perdikaris J, Turcotte R, Lafleur J, and Larouche B. 2017.

Probable maximum flood in a changing climate: and overview for Canadian basins. *Journal of Hydrology: Regional Studies* **13**: 11-25. DOI: 10.1016/j.ejrh.2017.07.003.

6. CWC (Central Water Commission). 2021. Guidelines for selecting and accommodating the inflow design floods for dams (Doc. No. CDSO_GUD_DS_06_v1.0). *Central Dam Safety Organisation*, Central Water Commission, Government of India, Dam Safety Rehabilitation Directorate, New Delhi. 210 pp.
7. Fattahi E, Noorian A M, and Noohi K. 2010. Comparison of physical and statistical methods for estimating probable maximum precipitation in southwestern basins of Iran. *DESERT (BIABAN)* **15 (2)**: 127 – 132.
8. Fernando W C D K, and Wickramasuriya S S. 2011. The hydro-meteorological estimation of probable maximum precipitation under varying scenarios in Sri Lanka. *International Journal of Climatology* **31 (5)**: 668-676. DOI: 10.1002/joc.2096.
9. Franks S W. 2002. Identification of a Change in Climate State Using Regional Flood Data. *Hydrology and Earth System Sciences* 6(1): 11-16. DOI: 10.5194/hess-6-11-2002
10. Franks S W, and Kuczera G. 2002. Flood frequency analysis: evidence and implications of secular climate variability, New South Wales. *Water Resources Research* **38 (5)**: 20.1 – 20.7. DOI: 10.1029/2001WR000232
11. Gurrapu S, St-Jacques J M, Sauchyn D J, and Hodder K R. 2016. The influence of the Pacific Decadal Oscillation on annual floods in the rivers of Western Canada. *Journal of the American Water Resources Association* **52 (5)**: 1031 – 1045. 10.1111/1752-1688.12433.
12. Gurrapu S, Sauchyn D J, and Hodder K R. 2022. Assessment of the hydrological drought risk in Calgary, Canada using weekly river flows of the past millennium. *Journal of Water and Climate Change*. DOI: 10.2166/wcc.2022.348
13. Kiem A S, Franks S W, and Kuczera G. 2003. Multi-Decadal Variability of Flood Risk. *Geophysical Research Letters* 30 (2): 1035. DOI: 10.1029/2002GL015992
14. Krishnamurthy L, and Krishnamurthy V. 2013a. *Influence of PDO on south Asian summer monsoon and monsoon-ENSO relation*. COLA Technical Report # 321. Centre for Ocean-Land-Atmosphere Studies. Institute of Global Environment & Society, Maryland, USA. 41 pp.
15. Krishnamurthy L, and Krishnamurthy V. 2013b. *Decadal scale oscillation and trend in the Indian monsoon rainfall*. COLA Technical Report # 322. Centre for Ocean-Land-

Atmosphere Studies. Institute of Global Environment & Society, Maryland, USA. 39 pp.

16. Kunkel K E, Karl T R, Easterling D R, Redmond K, Young J, Yin X, and Hennon P. 2013. Probable maximum precipitation and climate change. *Geophysical Research Letters* **40 (7)**: 1402-1408. DOI: 10.1002/grl.50334.
17. Kwon H-H, Brown C, and Lall U. 2008. Climate informed flood frequency analysis and prediction in Montana using hierarchical Bayesian modelling. *Geophysical Research Letters* **35 (5)**: L05404. DOI: 10.1029/2007GL032220.
18. Li Z, Lin X, and Cai W. 2017. Realism of modelled Indian summer monsoon correlation with the tropical Indo-Pacific affects projected monsoon changes. *Scientific Reports* **7**: 4929. 10.1038/s41598-017-05225-z
19. López J, and Francès F. 2013. Non-stationary flood frequency analysis in continental Spanish rivers, using climate and reservoir indices as external covariates. *Hydrology and Earth System Sciences* **17 (8)**: 3189-3203. DOI: 10.5194/hess-17-3189-2013.
20. Milly P C D, Betancourt J, Falkenmark M, Hirsch R M, Kundzewicz Z W, Lettermaier D P, and Stouffer R J. 2008. Stationarity is dead: Whither water management. *Science* **319 (5863)**: 573-574. DOI: 10.1126/science.1151915.
21. Ramak, Porhemmat J, Sedghi H, Fattahi E, and Lashni-Zand M. 2017. The climate change effect on probable maximum precipitation in the catchment. A case study of the Karun River catchment in the Shalu bridge site (Iran). *Russian Meteorology and Hydrology* **42**: 204 – 211. DOI: 10.3103/S10683739170 30086.
22. Roy S S, Goodrich G B, and Balling Jr. R C. 2003. Influence of El Niño/Southern Oscillation, Pacific Decadal Oscillation and local sea-surface temperature anomalies on peak season monsoon precipitation in India. *Climate Research* **25 (2)**: 171 – 178. DOI: 10.3354/cr025171.
23. Saini D, Bharadwaj P, and Singh O. 2022. Recent rainfall variability over Rajasthan, India. *Theoretical and Applied Climatology* **148 (1-2)**: 1 – 19. DOI: 10.1007/s00704-21-03904-6
24. Sajani S, Beegum S N, and Moorthy K K. 2007. The role of low-frequency intraseasonal oscillation in the anomalous Indian summer monsoon rainfall of 2002. *Journal of Earth System Science* **116 (2)**: 149 – 157. DOI: 10.1007/s12040-007-0015-5.

25. Stedinger J R, and Griffis V W. 2008. Flood Frequency Analysis in the United States: Time to Update. *Journal of Hydrologic Engineering* **13 (4)**: 199-204. DOI: 10.1061/(ASCE)1084-0699(2008)13:4(199)).
26. Stedinger J R, and Griffis V W. 2011. Getting from Here to Where? Flood Frequency and Climate. *Journal of the American Water Resources Association* **47 (3)**: 506-513. DOI: 10.1111/j.1752-1688.2011.00545.x.
27. Tan X, and Gan T Y. 2015. Nonstationary Analysis of Annual Maximum Streamflow of Canada. *Journal of Climate* **28 (5)**: 1788-1805. DOI: 10.1175/JCLI-D-14-00538.1.
28. Ward P J, Eisner S, Florke M, Dettinger M D, Kummu M. 2014. Annual flood sensitivities to El Niño-Southern Oscillation at the global scale. *Hydrology and Earth System Sciences* **18**: 47 – 66. DOI: 10.5194/hess-18-47-2014.
29. Wieland M. 2016. Safety aspects of sustainable storage dams and earthquakes of existing dams. *Engineering* **2 (3)**: 325-331. DOI: 10.1016/J.ENG.2016.03.011.
30. WMO (World Meteorological Organization). 1973. Manual on estimation of probable maximum precipitation (PMP). *Operational Hydrology Report No. 1 (WMO – No. 332).* Secretariat of the World Meteorological Organisation, Geneva, Switzerland.

APPENDICES

Table A1. Rank-based Spearman correlations (ρ) between annual peak flows in the selected gauges and the low-frequency atmosphere-ocean oscillations including Pacific Decadal Oscillation (PDO), El Niño-Southern Oscillation (ENSO), and Indian Ocean Dipole (IOD). The statistically significant correlations are bolded and the others are shown in Grey color.

		Spearman's ρ (Correlations between Annual Peak Flow and					
Station ID	**Data Length**	**PDO**	***p*-value**	**ENSO**	***p*-value**	**IOD**	***p*-value**
GPAC02	32	-0.41	**0.019**	0.23	0.201	0.23	0.212
GDHA03	47	-0.34	**0.021**	0.48	**0.001**	-0.20	0.288
GGRB04	38	-0.22	0.195	0.34	**0.037**	-0.16	0.384
GPUR05	45	-0.18	0.239	0.25	0.104	-0.31	**0.088**
GSAI06	47	-0.36	**0.013**	0.45	**0.002**	-0.45	**0.009**
GKAN07	25	-0.18	0.377	0.19	0.375	-0.07	0.731
GYEL09	36	-0.06	0.719	0.20	0.245	-0.22	0.235
GBET10	16	0.03	0.914	0.23	0.393	-0.55	**0.028**
GDEG11	27	-0.01	0.949	0.07	0.742	-0.27	0.166
GMAN12	25	-0.21	0.325	0.08	0.715	0.17	0.425
GHIV13	30	-0.33	**0.075**	-0.04	0.814	0.33	**0.078**
GGAN14	26	-0.27	0.188	0.47	**0.014**	-0.29	0.151
GPGB15	52	-0.20	0.157	0.23	**0.095**	-0.13	0.445
GNAN16	31	-0.41	**0.024**	0.12	0.508	0.12	0.522
GRAM17	31	0.02	0.925	-0.17	0.36	0.18	0.325
GSAT18	31	-0.06	0.729	-0.11	0.55	0.17	0.355
GBAM19	52	-0.08	0.594	0.21	0.13	0.18	0.301
GMAN20	49	-0.21	0.149	0.44	**0.001**	-0.31	**0.078**
GBHA21	31	-0.24	0.189	0.17	0.372	-0.18	0.332
GSIR22	47	-0.25	**0.092**	0.18	0.239	0.01	0.951
GRAJ23	31	-0.31	**0.093**	0.04	0.846	0.21	0.264
GZAR24	27	0.02	0.906	0.24	0.238	-0.41	**0.034**
GASH25	52	-0.35	**0.011**	0.33	**0.016**	-0.04	0.801
GSOM26	48	-0.16	0.29	0.39	**0.007**	-0.19	0.298
GKEO27	30	-0.15	0.415	0.13	0.501	-0.0007	0.997
GSAL28	31	-0.13	0.488	0.08	0.674	0.07	0.722
GTEK29	53	-0.25	**0.072**	0.36	**0.008**	0.09	0.609
GWAI30	25	-0.48	**0.015**	0.06	0.767	0.39	**0.053**
GRAJ31	31	-0.13	0.497	0.06	0.768	0.10	0.585
GPAT32	50	-0.24	**0.096**	0.19	0.189	0.08	0.649
GPER33	50	-0.34	**0.016**	0.38	**0.007**	-0.01	0.976
GSAN35	17	0.13	0.619	0.08	0.751	-0.29	0.264

GKUM37	31	-0.26	0.152	-0.05	0.778	0.10	0.598
GTUM38	24	-0.19	0.375	0.12	0.574	-0.11	0.607
GCHI39	44	-0.19	0.226	0.001	0.995	0.08	0.652
GKON40	50	-0.19	0.183	0.19	0.188	-0.10	0.597
GCHE41	18	0.19	0.505	-0.28	0.261	0.34	0.168
GPOL43	50	-0.25	**0.086**	0.32	**0.023**	-0.03	0.856
GAMB45	21	0.06	0.81	-0.09	0.695	0.15	0.518
GPOT46	17	0.16	0.541	-0.15	0.554	0.21	0.411
GSON47	23	0.03	0.883	-0.10	0.638	-0.04	0.854
GJAG48	49	0.02	0.888	0.13	0.358	0.01	0.973
GSAR49	45	-0.10	0.506	-0.07	0.631	0.08	0.648
GKOS50	18	0.11	0.669	-0.19	0.448	0.25	0.324
GMUR51	27	-0.09	0.658	-0.17	0.394	0.05	0.811
GNOW52	50	0.09	0.528	0.02	0.9	-0.06	0.72
NDIN01	28	0.24	0.224	-0.30	0.121	-0.06	0.744
NMOH02	39	0.11	0.517	-0.36	**0.023**	0.01	0.957
NMAN03	40	0.12	0.463	-0.34	**0.034**	0.08	0.646
NBAM04	17	0.45	**0.074**	-0.10	0.715	-0.03	0.918
NPAT05	37	0.13	0.446	-0.34	**0.041**	0.10	0.576
NBEL06	39	0.13	0.425	-0.44	**0.005**	0.21	0.226
NBAR07	45	-0.02	0.895	-0.16	0.307	0.05	0.761
NGAD08	39	-0.05	0.771	-0.16	0.329	0.16	0.358
NSAN09	38	0.08	0.613	-0.31	**0.06**	0.15	0.4
NHOS10	44	-0.06	0.701	0.03	0.824	0.10	0.585
NCHH11	40	-0.06	0.691	-0.09	0.584	-0.03	0.852
NHAN12	39	-0.08	0.613	0.02	0.896	0.11	0.533
NKOG13	40	0.04	0.811	-0.06	0.723	0.19	0.274
NMAN14	46	-0.11	0.464	0.15	0.327	0.11	0.515
NDHU15	16	0.30	0.259	-0.45	**0.083**	0.15	0.572
NPAT16	16	-0.16	0.564	-0.14	0.594	-0.13	0.641
NGAR17	44	-0.13	0.419	0.32	**0.035**	0.002	0.987
NCHA18	37	-0.28	**0.096**	0.17	0.314	-0.08	0.659

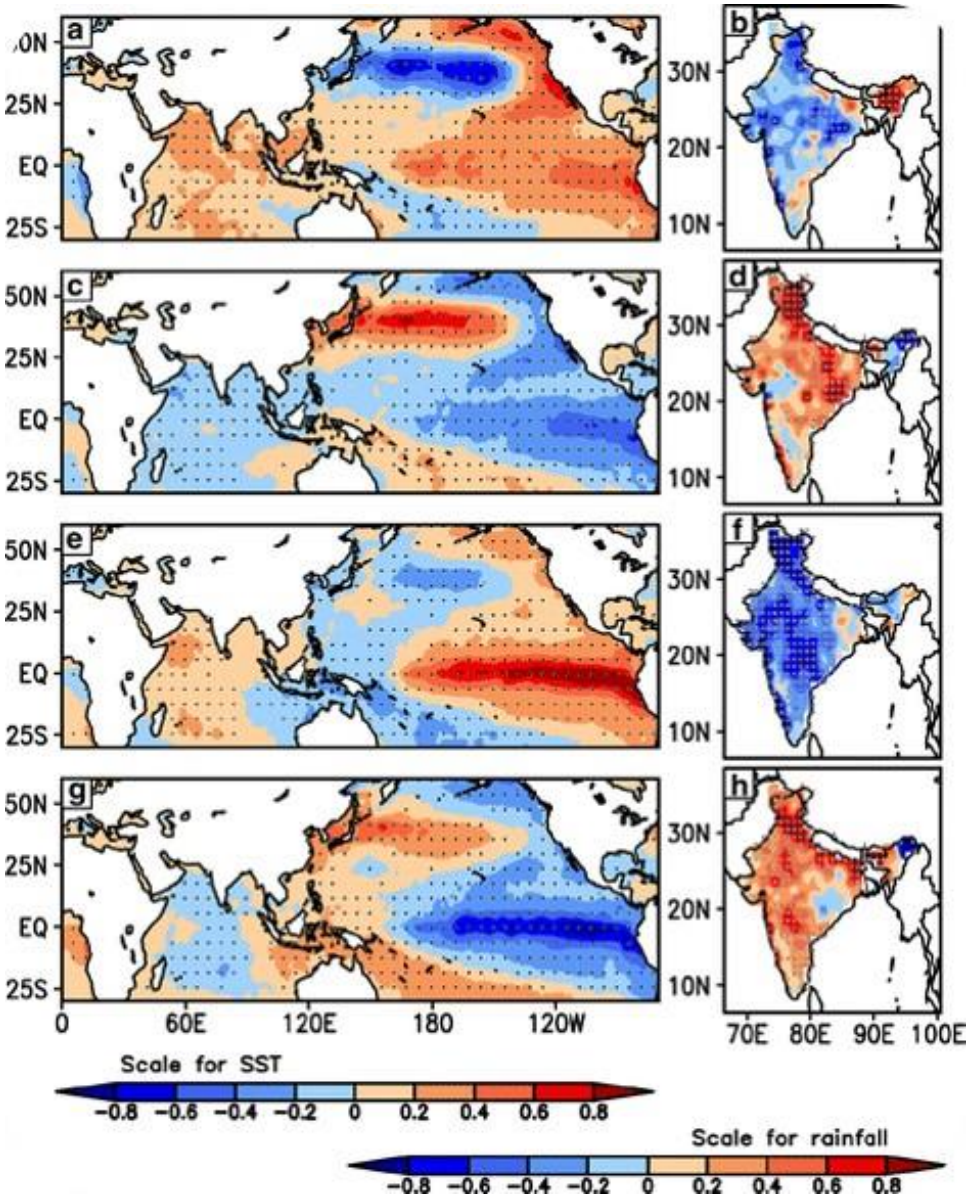

Figure A1. The influence of low-frequency PDO and ENSO on Indian Summer Monsoon Rainfall (ISMR). (a) Higher sea surface temperature (SST) across equatorial Pacific Ocean indicate positive phase of PDO can be associated with the (b) below normal rainfall and relatively (c) lower SST across equatorial Pacific Ocean can be associated with the (d) above normal rainfall across India. Similarly, (e) positive episodes of ENSO (El Niño) can be associated with (f) below normal rainfall and (g) negative episodes of ENSO (La Niña) can be associated with (h) above normal rainfall across India. (Figure Source: Krishnamurthy & Krishnamurthy, 2013a)